Applied Geochemistry 31 (2013) 60–78

Contents lists available at SciVerse ScienceDirect

Applied Geochemistry

journal homepage: www.elsevier.com/locate/apgeochem

Control of early diagenesis processes on trace metal (Cu, Zn, Cd, Pb and U) and metalloid (As, Sb) behaviors in mining- and smelting-impacted lacustrine environments of the Bolivian Altiplano

Joseline Tapia [a,b,c], Stéphane Audry [a,*]

[a] Université de Toulouse, OMP-GET, 14 Avenue Edouard Belin, 31400 Toulouse, France
[b] Departamento de Geología, Universidad de Chile, Plaza Ercilla 803, Casilla 13518, Correo 21, Santiago, Chile
[c] Escuela de Ciencias de la Tierra, Universidad Andres Bello, 7 Norte 1348, Viña del Mar, Chile

ARTICLE INFO

Article history:
Received 24 February 2012
Accepted 18 December 2012
Available online 11 January 2013
Editorial handling by G. Bird

ABSTRACT

A combination of mineralogical (SEM–EDS, EMPA) and geochemical (redox dynamics, selective extractions) approaches was applied to mining- and smelting-impacted sediments from Lake Uru Uru and from the Cala Cala Lagoon, a non-impacted reference site, in the Bolivian Altiplano. The purpose was to assess the factors controlling the post-depositional redistribution (mobilization/sequestration) of trace metals and metalloids. As expected, trace metals and metalloids are less reactive at the reference site than in Lake Uru Uru. In the latter, trace metals and metalloids are principally hosted by Fe- and Mn-oxyhydroxides, authigenic sulfides and silicate particulates. Post-depositional redistribution is ascribed to early diagenetic processes driven by organic matter (OM) mineralization, including dissolution of trace metal-bearing phases and precipitation of authigenic sulfide and carbonate phases. Seasonal climate variability exerts a strong influence on these processes. Evaporation of surface water during the dry season in the northern part of Lake Uru Uru promotes large redox front oscillations in the sediments and, therefore, transient redox conditions, likely leading to the weakening of anoxia in near-surface sediments and to a 'compressed' redox zonation compared to the southern part of the lake. Seasonal disappearance of the water column in the Northern Lake Uru Uru entails an alternation of: (i) low trace element mobility in the dry season due to elemental precipitation; and (ii) an increase of trace element mobility via diffusive transport during the wet season due to release from OM, Fe- and Mn-oxyhydroxides and carbonates upon mineralization, reductive dissolution and destabilization processes, respectively. Reoxidation of authigenic Fe-sulfides likely following the re-instalment of the water column above the sediment at the end of the dry season and prior to the return of anoxia probably favors transport of trace elements to the water column. As a consequence of this intricate web of redox- and climate-related processes, both northern and southern sediments of Lake Uru Uru are a source of dissolved trace elements, particularly As and Cd, for the overlying water column via diffusive transport. However, much of the diffused As and Cd is likely to be removed from the dissolved phase by the redox loop through Fe-oxyhydroxide precipitation. Finally, it is suggested that long term sequestration of trace metals and metalloids in the sediments could be controlled by inter-annual climate variability such as ENSO events.

1. Introduction

In the idealized steady-state view of early diagenesis, a sediment deposit is characterized by defined zones within which only specific redox reactions can take place (Froelich et al., 1979). However, in reality redox boundaries between zones appear generally blurred (e.g., Aller et al., 2004; Audry et al., 2006b, 2010). That observation holds for continental environments (e.g. lakes and reservoirs) and, therefore, one can consider sediments as being characterized by unsteady redox conditions and behaving like a batch reactor (Aller, 2004). Unsteady redox conditions are generally driven by temporal variations in organic C input, sedimentation rate, temperature and chemical composition of the overlying water column (WC). This causes fluctuations in the depth of the oxic–anoxic boundary, creating zones where redox-sensitive elements (such as trace metals and metalloids) are alternately oxidized and reduced and where sulfides are alternately precipitated and dissolved (Gobeil et al., 1997). During early diagenesis, part of the organic matter (OM) deposited in sediments is mineralized close to the water–sediment interface (WSI), with O_2, NO_3^-, Fe- and Mn-oxyhydroxides or SO_4^{2-} acting as electron acceptors (Froelich et al., 1979; De Lange,

* Corresponding author. Tel.: +33 5 61 33 26 05.
E-mail address: stephane.audry@get.obs-mip.fr (S. Audry).

0883-2927/$ - see front matter © 2013 Elsevier Ltd. All rights reserved.
http://dx.doi.org/10.1016/j.apgeochem.2012.12.006

1986). When surface sediments are enriched in Mn- and/or Fe-oxyhydroxides and are characterized by high physical or biological mixing rates, Fe and Mn reduction coupled to OM oxidation typically become geochemically important (Aller, 1990, 1994). The coupling is either direct, with Mn- and Fe-oxyhydroxides acting as electron acceptors in the mineralization of organic material (Aller, 1990), or indirect, with Mn- and Fe-oxyhydroxides acting as intermediates between, for instance, sulfide produced during SO_4^{2-} reduction and oxidation by O_2 (Aller, 1994).

Early diagenetic processes have been widely and intensively studied and documented in marine environments (e.g., Allen et al., 1990; Calvert and Pedersen, 1993; Laslett and Balls, 1995; Rosenthal et al., 1995; Slomp et al., 1997; Morford and Emerson, 1999; Tang et al., 2002; Whiteley and Pearce, 2003; Sundby et al., 2004; Morford et al., 2005;Audry et al., 2007; Soto-Jiménez and Páez-Osuna, 2008) through either field studies (e.g., Postma and Jakobsen, 1996; Van Cappellen et al., 1998; Hyacinthe et al., 2001; Hyacinthe and Van Cappellen, 2004) or multi-component reactive-transport diagenetic modelling (e.g., Tromp et al., 1995; Wang and Van Cappellen, 1996). However, while such studies continue to be published (e.g., Huerta-Diaz et al., 1998; Granina et al., 2004; Audry et al., 2006b, 2010; Canavan et al., 2007; Lesven et al., 2008), our knowledge of early diagenesis in freshwater environments remains patently fragmentary. Studies of processes related to post-depositional redistribution of trace metals and metalloids in continental aqueous systems, such as lakes, and their relationships with temperature, pore water chemistry, overlying WC composition, among other factors, are still limited (Petersen et al., 1997; Audry et al., 2010), making it difficult to understand factors that control trace metal and metalloid mobility and impacts on these environments.

Evidence that pore water properties can fluctuate significantly is mostly limited to environments that are subjected to seasonal temperature variations (e.g., Aller, 1994). Extreme (inter)annual fluctuations are characteristic of the Bolivian highlands. This area experiences periodic droughts (due to both rain scarcity and high evaporation rates) and floods (UNEP, 1996; Garcia Moreno, 2006) and has a lower partial pressure of O_2, given the high average altitude (3600–4200 m a.s.l.). To the authors' knowledge, no studies have yet assessed the factors and processes that control the post-depositional redistribution of trace metals and metalloids in high altitude tropical environments affected by periodic dessication such as the Bolivian Altiplano. The growing impact of anthropogenic activities such as mining and smelting in this region (Tapia et al., 2012) reinforce the need to improve our understanding of post-depositional aquatic sedimentary geochemistry in high-altitude settings.

The present study contributes to that need and is based on the sampling of a total of five lacustrine sediment cores from the Bolivian Altiplano. The aim of the research was to document early diagenetic oxidation–reduction processes in order to assess their impact on the post-depositional redistribution of Fe, Mn, and trace elements (Cu, Zn, Pb, Cd, U, As, Sb) and the potential consequent upward diffusive fluxes to the overlying WC. The cores were retrieved from an Altiplanic lacustrine environment heavily impacted by mining and smelting activities during different seasons and, for comparison, (ii) from a non-anthropogenically impacted mountainous lake. Based on high-resolution (mm-scale) vertical profiles of dissolved, total and selectively-extracted particulate trace metals and metalloids, and redox-sensitive elements (N-species, SO_4^{2-}, Fe and Mn), a conceptual model is proposed of trace metal and metalloid behavior during early diagenesis within contaminated lakes and a non-impacted lake of the Bolivian Altiplano. The importance of seasonal climate variability is stressed, especially evaporation of the water column and its impact on the studied ecosystems during the dry season.

2. Background and methods

2.1. The Altiplano of Oruro, TDPS and Altiplanic lakes

Oruro Department is located within the Altiplano of Bolivia, a 200,000 km^2 intermontane basin formed during the Pliocene and Early Pleistocene (some 2–3 Ma), in the central Andes of Peru, Bolivia and Argentina (Lavenu et al., 1984). This basin is bounded to the west by the Western Andes Cordillera and to the east by the Eastern Andes Cordillera, both characterized by highly mineralized geomorphological features characterized by ore mineralization associated with redbed Cu deposits and epithermal deposits in the altiplano and Western Cordillera; and the Sn belt, the Au–Sb belts, and the Pb–Zn belt in the Eastern Cordillera (Arce-Burgoa and Goldfarb, 2009; Tapia et al., 2012).

The main hydrological system of the Altiplano corresponds to the endorheic Lake Titicaca-Desaguadero River–Lake Poopó-Coipasa Salar (TDPS; Fig. 1). This area has dry (DS) and wet seasons (WS) extending from May to September and October to March, respectively. Despite scarcity of precipitation (<400 mm; UNEP, 1996), intermittent flood periods have affected the Altiplano, with great floods observed during 1921, 1930–1935, 1964, 1985, 1987 (Garcia Moreno, 2006). These floods were associated with cold El Niño Southern Oscillation (ENSO) events (La Niña), which have influenced historical lacustrine levels since the early Pleistocene (PPO, 1993–1996; PPO-9606, 1996). In contrast, droughts in the region are associated with warm ENSO (El Niño) events. Significant droughts have occurred during modern times in 1937, 1944, 1947, 1956, 1967–1968, 1983, 1988 (Garcia Moreno, 2006).

2.2. Sample collection and handling

Lake Uru Uru (150 km^2) is located north of Lake Poopó and belongs to the TDPS system. It is a shallow lake that formed during the 1900s due to the deviation of the Desaguadero River and is divided by a railroad and a highway embankment, allowing minimum exchange of water between the two separate parts (Fig. 1). The western part is fed by the eastern branch of the Desaguadero River and by the Thajarita River. The northern part (90 km^2) is fed by the Tagarete River, a channelized water course (Fig. 1). The southern part (60 km^2) is drained through the Desaguadero River, flowing south for ca. 30 km before entering Lake Poopó. The Kori Kollo open-pit mine and associated waste rock dump are located proximal to the Desaguadero River. The San Juan de Sora Sora River enters the basin from the east, transporting its waters into the southern outflow of Lake Uru Uru (up to 7 km to the south); this river drains the Huanuni and Santa Fé river basins. The Huanuni River receives direct dumping of the untreated tailings of the state-owned Huanuni Sn mine. The northern part of Lake Uru Uru is periodically subjected to dessication due to shallowness, scarcity of precipitation and high evaporation rates while the southern part has a permanent WC. Another contrast between the two parts of the lake is the high density of sedge (*Schoenoplectus totora*), grass (*Ruppia*) and algae (*Chara*) in the southern part compared to the north. The Cala Cala Lagoon (1.5 km^2) is located within the Eastern Andes Cordillera and is drained by the Khala Khala River (Fig. 1). Sampling of sediment cores from Lake Uru Uru and Cala Cala Lagoon was conducted in April 2008 and February 2009. During these coring campaigns, the northern and southern areas of Lake Uru Uru were sampled during DS (21st–25th of April 2008) and WS (2nd–6th of February 2009). Both areas are affected by past mining (Tapia et al., 2012). Additionally, the Cala Cala Lagoon, located in an area not impacted by mining Tapia et al., 2012), was sampled during the WS (2nd–6th of February 2009) for comparison (Fig. 1). During these sampling

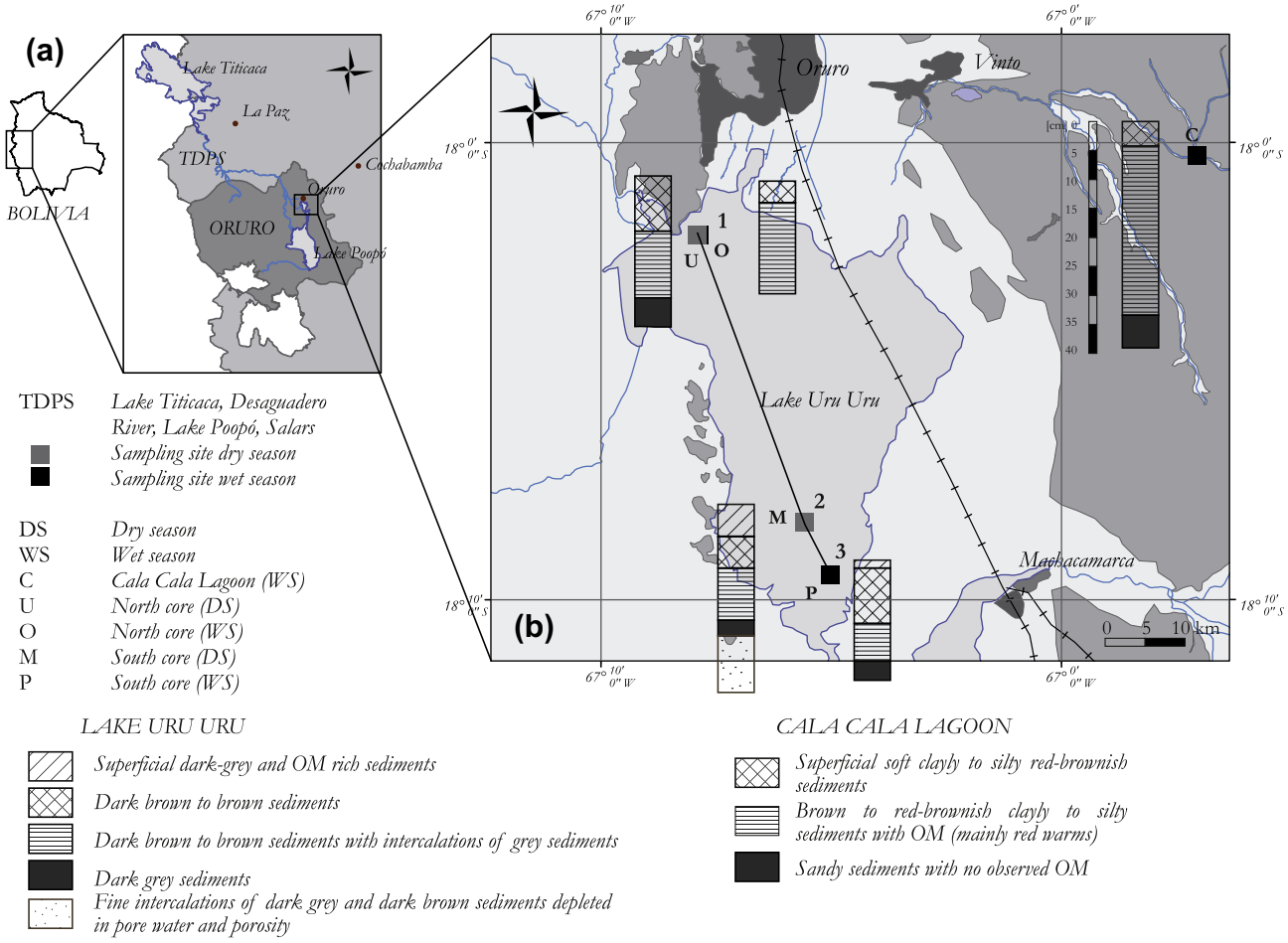

Fig. 1. TDPS endorheic hydrological system (a) and the sediment sampling sites (b). OM, organic matter; DS, dry season; WS, wet season.

campaigns five sediment cores were retrieved. Sampling was done using a Large Bore Interface Corer (Aquatic Research Instruments®) equipped with a polycarbonate core tube (60 cm length, 10 cm inner diameter). This corer enables sampling the uppermost decimetres of the sediments without any disturbance of the WSI. Immediately after recovery, bottom water (BW) was sampled from the undisturbed WSI of the core using a 20-mL syringe, then filtered through cellulose acetate syringe filters (0.2 μm porosity; Nalgene®) and divided into three aliquots for nutrient, SO_4^{2-} and Cl^-, and metal/metalloids analyses. Aliquots for nutrient, SO_4^{2-} and Cl^- analyses were stored at −20 °C until analysis; aliquots for metal and metalloid measurements were acidified (pH ~ 1; HNO_3 ultrapure 1‰) and stored in acid-cleaned tubes at 4 °C.

Cores were subsequently extruded and sliced with an acid-cleansed plastic cutter (see details in Tapia et al. (2012)) with a vertical resolution of 5 mm near the water–sediment interface to 2 cm near the bottom of the core. Sediment slicing was open-air operated in order to avoid sediment warming, partial drying of the sections and water advection that occur when an insulating device (O_2-free glove box) is used due to much longer core processing time (ca. 5 h compared to less than 60 min with the open-air protocol). With the open-air protocol, the part of the sediment in contact with the atmosphere is the top of the slice when the previous slice has been sampled. It is estimated that the average time of contact between the top of the processed slice and atmospheric O_2 is ca. 2 min. During this period of time, it was estimated that less than 0.1% of the slice's volume could be affected by O_2 contamination. It is, therefore, possible that vertical distribution of dissolved elements that are soluble when oxidized and non-soluble when reduced, such as U, would be slightly affected (Chaillou et al., 2002). All sediment samples were immediately collected in acid-cleaned 200-mL propylene centrifuge vials, N_2-flushed and centrifuged at 4000 r.p.m. for 20 min. For each sample, the supernatant (i.e. porewater) was processed and stored similarly to BW samples. The sediment samples were then N_2-flushed and sealed in sample bags.

2.3. Porewater analysis

Sulfate, Cl^- and NO_3^- concentrations were determined by ion chromatography with a Dionex ICS 2000 Chromatograph. The detection limits (DLs) for SO_4^{2-}, Cl^- and NO_3^- were 0.02, 0.04 and 0.002 mg L^{-1}, respectively. Accuracy was better than 5% and reproducibility better than 3%. Ammonium was determined by ion chromatography with a Dionex ICS 1000 Chromatograph, accuracy was better than 5%.

2.4. Trace metal and metalloid measurements

Total dissolved and particulate trace metal and metalloid concentrations were measured using a quadrupole ICP-MS 7500 ce. (Agilent Technologies). The analytical methods employed were quality checked by analysis of certified international reference water (SLRS-4). Sediment total digestion included method blanks and digestion of certified international reference materials (LKSD-1 and LKSD-3). Accuracy was within 5% of the certified values and the analytical error (rsd) generally better than 10% for concentrations 10 times higher than the detection limits.

Concentrations of Mn subjected to exchangeable (Mn_{MgCl2}) and ascorbate (Mn_{asc}) digestions were measured with ICP-OES (Ultima 2 from Horiba Jobin Yvon). Analytical error (rsd) was <5% for Mn_{MgCl2} and <2% for Mn_{asc}.

2.5. Characterization of the solid material

Granulometry was determined using a laser granulometer (2.0 Mastersizer 2000). Particulate organic C (POC), total C (C_{tot}) and total S (S_{tot}) were measured on the dry, powdered and homogenized material using a carbon/sulfur analyzer (Horiba Jobin Yvon Emia-320 V C/S Analyser). Inorganic C was eliminated by HCl addition prior to analysis of POC. Particulate inorganic C (PIC) was calculated by subtracting POC from C_{tot}.

Single chemical extractions (i.e., using a separate aliquot of the same sample for each reagent) were applied on all sediment samples. The single extraction procedures used in this study were principally based on the sequential extraction scheme of Tessier et al. (1979). Previous studies (e.g., Tack et al., 1996, 1999; Alborès et al., 2000) have shown that similar results for trace metal partitioning (Cu, Cr, Ni, Pb, and Zn) were obtained from the conventional sequential extraction method (Tessier et al., 1979) and from single extractions using identical operating conditions applied in each individual extraction. Single extractions were chosen over sequential extractions in order to avoid (1) possible changes in elemental speciation during the successive extraction steps, (2) changes or losses of elemental species during the residue washing step (Rosenberg and Ariese, 2001) and (3) multiple risks of sample contamination from the successive reagents used (Quevauviller, 1998). Similar single selective extractions have been successfully applied in previous studies of mining- and smelting-impacted aquatic systems (e.g., Audry et al., 2006a, 2010). The single extraction protocols and the five operationally-defined target fractions are presented in Table 1. The residual fraction (R) was estimated as the difference between the total metal content (TMC) and the sum of the fractions F1 + F2 + F3 + F4. The contribution of each operationally-defined fraction in a sample is expressed as a percentage of the TMC. It will be shown later that, in some cases and particularly for Mn and Cd, the most reactive phases were non-selectively extracted (i.e. F1 + F2 + F3 + F4 > TMC) by the conventional extractants used here. Such a drawback has been reported previously by Audry et al. (2006a) in a similarly mining-impacted freshwater system. It should be noted that these selectivity problems could not have been proved if sequential extraction was used. Nevertheless, qualified but interesting information on trace element mobility can be drawn from these results.

Mineralogical determinations were performed on Lake Uru Uru sediments by scanning electron microscopy (SEM), using an accelerating voltage of 20 kV, equipped with an X-ray energy-dispersive spectral analyzer (EDS) and electron microprobe. Detailed observations using SEM were performed on selected (based on TMC) sediment samples exposed on the surface of cylindrical epoxy plugs that were covered with a 20–50 nm thick carbon film before analytical observation; analyses were performed under accelerations between 15 and 20 kV. During the observations, SEI mode images yielded morphologies of the minerals in the sample, while the BEC mode allowed characterization of samples as a function of their chemical composition. Selected minerals observed through SEM were analyzed by electron microprobe (Cameca SX50) to determine the chemical composition of sulfides and oxides. Acceleration tension was c. 15 kV for oxides and c. 25 kV for sulfides. For sulfides and oxide, beam size was $2 \cdot 2$ μm with a current of 20 nA.

2.6. Diffusive fluxes

Diffusive fluxes through the WSI were determined following Fick's first law.

$$Jsed = -\phi Dsed\left(\frac{\partial C}{\partial z}\right) \quad (1)$$

where *Jsed* (μmol cm^{-4}) is the diffusive flux in the sediment, ϕ porosity, *Dsed* is the diffusive coefficient in sediment and $\partial C/\partial z$ is the linear concentration gradient through the WSI. Values for *Dsed* were calculated on the basis of a dimensionless tortuosity (θ^2) and the diffusion coefficient in free solutions (D_0) following $Dsed = D_0/\theta^2$ (cm^2 s^{-1}). Dimensionless tortuosity was determined by $\theta^2 = 1 - \ln(\phi^2)$ (Boudreau, 1996). Values of D_0 were based on experimental data from Li and Gregory (1974) and corrected for temperature (15 °C). *Dsed* was not corrected for any random transport mechanism such as biodiffusion, gas ebullition or wave-induced mixing. For As, Sb and U, *Dsed* was estimated using the molecular self-diffusion coefficient (D_0) for the arsenate, antimonate and UO_2 species (Widerlund and Ingri, 1995). Positive *Jsed* indicates an upward-directed flux (efflux from the sediment into the overlying water column) and negative *Jsed* indicates a downward-directed flux (influx from the water column into the sediment).

3. Results

3.1. Solid phase

3.1.1. Water content, porosity and granulometry

All five sediment cores are characterized by decreasing water content and porosity with depth (Table 2) due to compaction.

Table 1
Operating conditions applied for single extraction procedures. DS, dry season; WS, wet season.

Fraction	Sample weight (mg)	Reagent	Shaking time, temperature	References
• F1 – Exchangeable	200	$MgCl_2$ 1M (pH = 7)	1 h at 25 °C	Tessier et al. (1979)
• F2 – Carbonate	500	10 mL NaOAc 1M + HOAc (pH = 5) pH adjustment with HOAc 5M during extraction	5 h at 25 °C	Tessier et al. (1979)
• F3 – Fe- and Mn-oxyhydroxides (reducible)	200	12.5 mL ascorbate solution (pH = 8)	24 h at 25 °C	Kostka and Luther (1994)
• F4 – Organic matter/sulfides (oxidizable)	200	1.6 mL H_2O_2 30% m/v + NaOH (pH = 5)	2 h at 85 °C	Tessier et al. (1979) modified
		Then 0.6 mL H_2O_2 30% m/v + NaOH	2 h at 85 °C	by Ma and Uren (1995)
		Then 1 mL NH_4OAc 1M + 0.8 mL H_2O milli-Q	30 min at 25 °C	
• TMC – Total metal content	30 (DS)	HCl 12N + HNO_3 14N + HF 26N	2 h at 110 °C (hotplate)	Schäfer et al. (2002) modified
		Then HCl 12N + HNO_3 14N	2 h at 110 °C (hotplate)	
	100 (WS)	HF 26N + HNO_3 14N + H_2O_2 30%	20 min at 150 °C (microwave)	EPA 3052

Table 2
Water content, porosity, particulate organic carbon (POC), particulate inorganic carbon (PIC), total sulfur (S_{tot}) and granulometry in the Cala Cala Lagoon and Lake Uru Uru sediments. DS, dry season; WS, wet season.

		Water content (%)	Porosity (%)	POC (%)	PIC (%)	S_{tot} (%)	Granulometry (%) Clay <2 μm	Silt 2–63 μm	Sand 0.063–1 mm
Cala Cala Lagoon	Mean	42	65	1.81	0.04	0.05	7	14	79
	Median	42	65	1.72	0.05	0.05	7	13	80
	Range	31–54	55–76	1.45–2.30	0.00–0.13	0.03–0.08	1–35	1–25	65–98
North. Uru Uru DS	Mean	42	66	1.14	0.72	0.21	–	–	–
	Median	43	66	0.98	0.71	0.18	–	–	–
	Range	34–48	58–71	0.74–1.57	0.14–1.42	0.07–0.38	–	–	–
North. Uru Uru WS	Mean	38	62	0.82	0.28	0.11	24	41	35
	Median	43	66	0.83	0.28	0.1	26	43	31
	Range	33–64	56–83	0.72–0.91	0.08–0.43	0.07–0.19	16–30	31–47	26–53
South. Uru Uru DS	Mean	53	74	2.12	0.75	1.1	–	–	–
	Median	48	71	1.05	0.59	1.3	–	–	–
	Range	37–86	61–94	0.49–6.04	0.00–2.36	0.08–1.62	–	–	–
South. Uru Uru WS	Mean	45	67	2.68	1.1	1.08	–	–	–
	Median	41	65	1.4	0.87	1.38	–	–	–
	Range	31–81	54–92	0.90–6.51	0.14–2.54	0.14–1.58	–	–	–

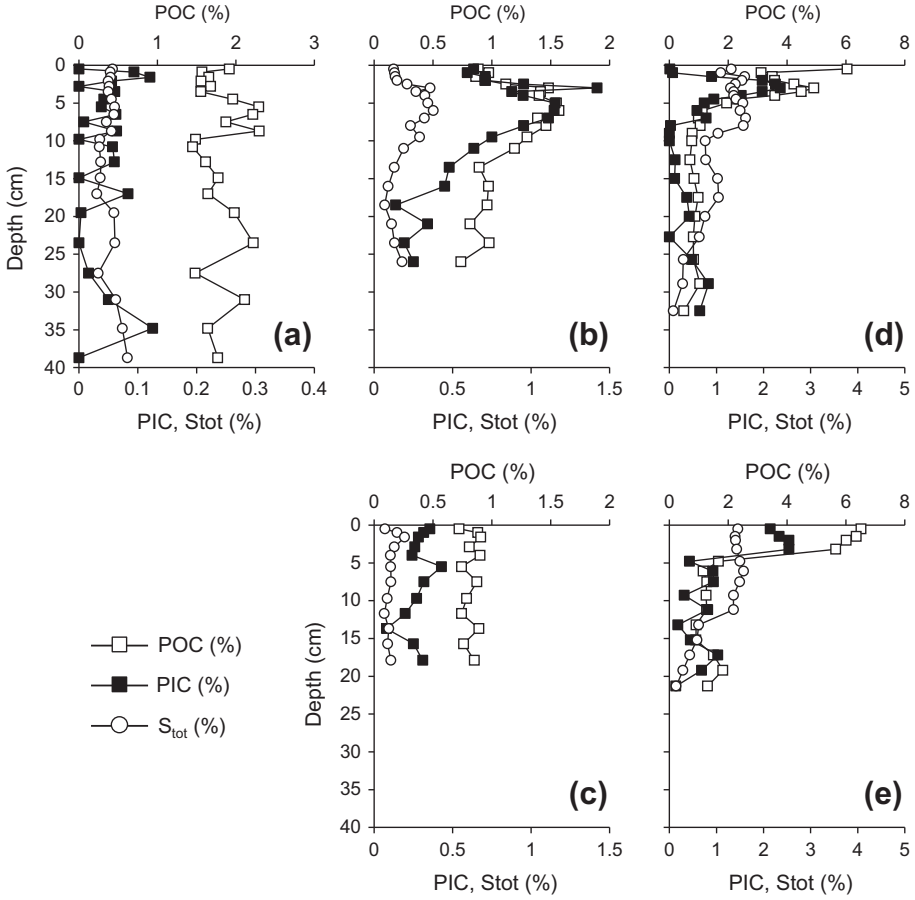

Fig. 2. Concentration–depth profiles of particulate organic (POC) and inorganic (PIC) C and total S (S_{tot}) in the sediments of Cala Cala Lagoon (a), Northern Lake Uru Uru in dry (b) and wet (c) season and Southern Lake Uru Uru in dry (d) and wet (e) season.

Granulometry was determined only for WS sediments in the Cala Cala Lagoon and Northern Lake Uru Uru (Table 2). Sand dominates in the Cala Cala Lagoon (79%), while there is a lesser occurrence of silt and clay (14% and 7%, respectively). Particle size proportions in Northern Lake Uru Uru are silt (41%), sand (35%) and clay (24%). Silt contents are constant within the depth profile, while sand is present mostly in the upper part of the core and clay tends to increase with depth (from 17% at the top to 30% at the bottom of the core).

3.1.2. Particulate organic carbon and total sulfur

The sediments of the Cala Cala Lagoon exhibit variable POC contents, with concentrations ranging from 1.5% to 2.3% (Fig. 2

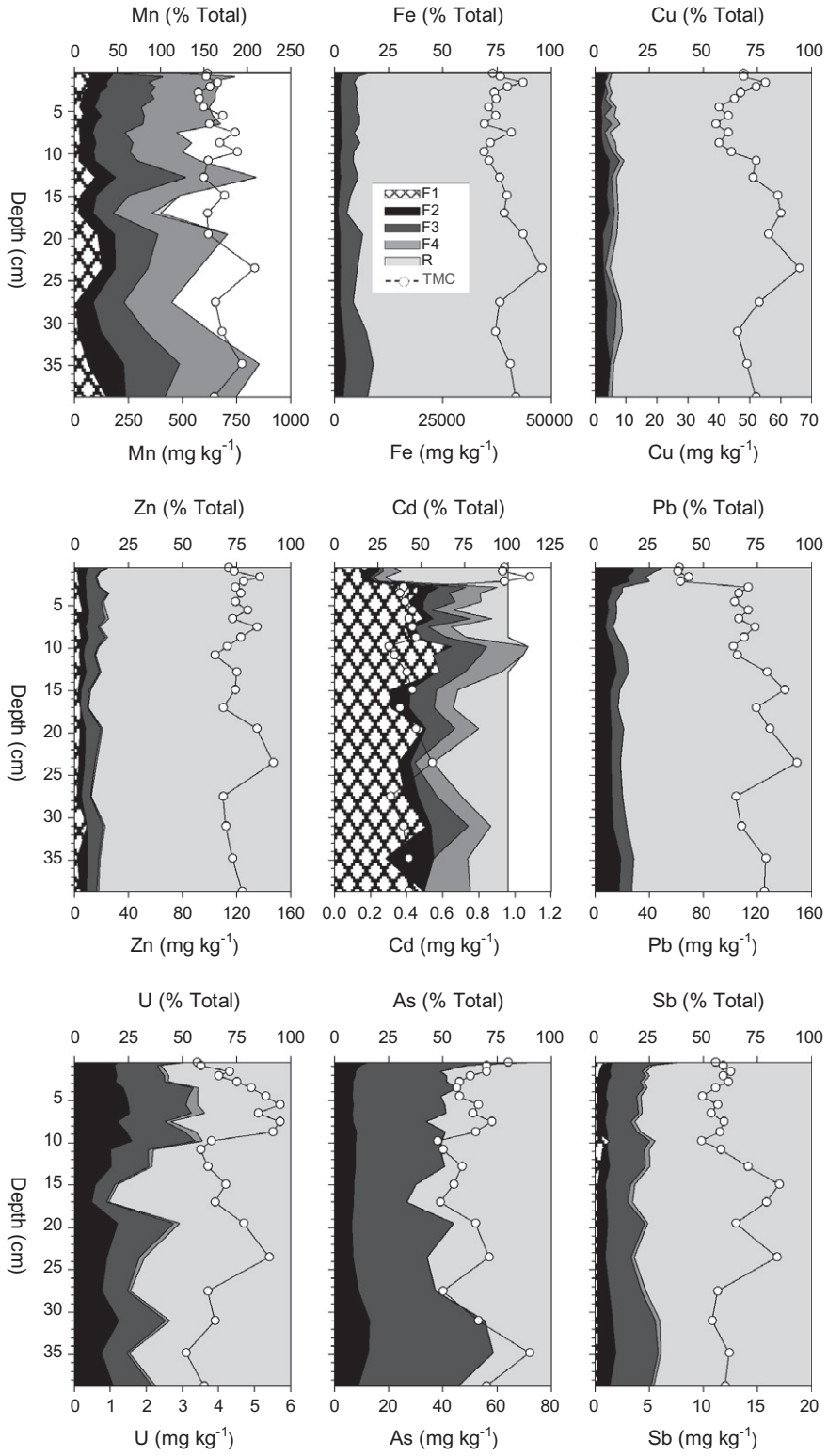

Fig. 3. Solid-state partitioning and total metal(loid) content (TMC) in the sediments of the Cala Cala Lagoon.

and Table 2). POC contributes to 98% of C_{tot} on average. Total S shows relatively low concentrations, decreasing from 0.06% to 0.03% in the first 17 cm below the WSI and then increasing up to 0.08%. The northern and southern parts of Lake Uru Uru have different particulate C and S concentrations and profile patterns (Fig. 2 and Table 2), with higher POC, PIC and S_{tot} average concentrations observed in the southern part. In the northern part, POC contributes up to 60% (DS) and 74% (WS) of C_{tot} on average and during the DS shows increasing concentrations below the WSI and then decreasing concentrations toward the bottom of the core. Constant POC concentrations with depth are observed during the WS. Total S is characterized by similar profiles in the DS and the WS and with profile patterns similar to that of POC (DS and WS) and PIC (DS). In the southern core, POC, PIC and S_{tot} show similar

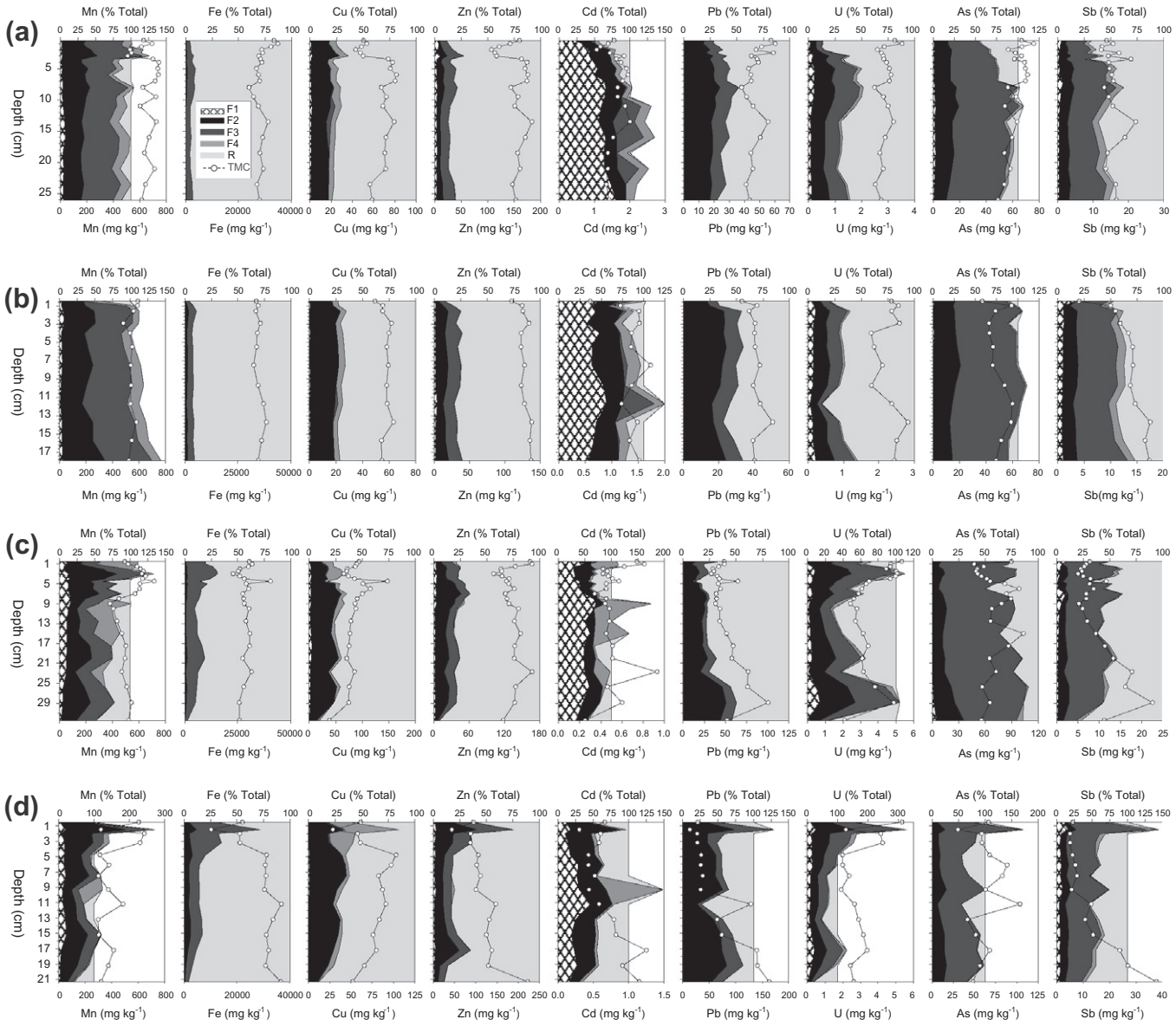

Fig. 4. Solid-state partitioning total metal(loid) content (TMC) in the sediments of the Northern Lake Uru Uru in dry (a) and wet (b) season and Southern Lake Uru Uru in dry (c) and wet (d) season.

trends, with decreasing concentrations with depth for both seasons. POC average contributions to C_{tot} (i.e. 71% for WS and 74% for DS) are comparable to those of the northern core.

3.1.3. Total particulate metals and metalloids

Total particulate Fe and Mn contents are more or less constant in the Cala Cala Lagoon and Lake Uru Uru (Fig. 3). The mean Fe concentration is 38,700 ± 3300 mg kg^{-1} for the Cala Cala Lagoon, 31,000 ± 3700 mg kg^{-1} (28,700 ± 2550 mg kg^{-1} in DS and 34,840 ± 1700 mg kg^{-1} in WS) and 28,500 ± 4900 mg kg^{-1} (28,530 ± 2770 mg kg^{-1} in DS and 28,420 ± 7290 mg kg^{-1} in WS) for northern and southern Lake Uru Uru, respectively. Mean Mn concentrations are 657 ± 68 mg kg^{-1}, 614 ± 80 mg kg^{-1} (654 ± 73 mg kg^{-1} in DS and 547 ± 31 mg kg^{-1} in WS) and 486 ± 114 mg kg^{-1} (531 ± 17 mg kg^{-1} in DS and 411 ± 126 mg kg^{-1} in WS) for the Cala Cala Lagoon, Northern and Southern Lake Uru Uru, respectively (Table 3). However, the upper parts of all cores exhibit significant variations in concentrations (Figs. 3 and 4) reflecting the time- and intensity-related variability of particle inputs to the basins.

Enrichment factors (EFs) estimated by Tapia et al. (2012) for the whole area demonstrated that metalloids such as As and Sb are significantly enriched compared to the upper continental crust (UCC). However, EFs calculation based on the average composition of the Cala Cala Lagoon sediments, the reference site, shows an order of magnitude lower EFs for both elements (Table 3). Mean enrichment factors for Lake Uru Uru's sediments calculated using the Cala Cala Lagoon Average Composition (CCLAC; Table 3) show values of at least 2 (up to 4 and 5 for As and Cd, respectively) for all the studied metals; only Pb is not significantly enriched in Lake Uru Uru compared to the Cala Cala Lagoon. These observations were discussed by Tapia et al. (2012). Therefore, higher background levels can be inferred than those found for the UCC and that the Altiplano sediments show peculiar characteristics related to the region's high degree of mineralization (Table 3). In addition, particulate trace metal and metalloid depth profiles are characterized by highly variable concentrations, especially in the sediments from southern Lake Uru Uru (Fig. 4 and Table 3), where standard deviations range to more than

40% and 70% of the mean during DS (Sb 49%) and WS (Pb 77% and Sb 84%) respectively.

3.1.4. Solid state partitioning

In the Cala Cala Lagoon (Fig. 3), Fe shows low reactivity, being mainly present in the residual fraction (~90% on average) likely in the form of crystalline Fe-oxides (goethite and hematite) and incorporated in silicate minerals. Operationally-defined reactive Fe is mostly found in the reducible fraction (F3; ~8% on average). This suggests that reactive Fe is mainly associated with amorphous oxides and/or oxyhydroxides. In contrast to Fe, Mn is more extractable, with F1 + F2 + F3 + F4 > 100% and with reactive Mn mainly distributed between the reducible (F3) and oxidizable (F4) fractions (Fig. 3). This is likely related to the fact that Mn is generally associated with poorly ordered phases and occurs in different valence states, particularly in systems impacted by mining/smelting activities (Lee et al., 2002). In the Cala Cala Lagoon, the most extractable (mobile) trace metals and metalloids are Cd (F1 + F2 + F3 + F4 = 74% on average), As (53%) and U (43%), while the less mobile are Cu (8%), Zn (13%), Pb (15%) and Sb (24%).

Overall, mineral phases carrying trace metals and metalloids are more readily extractable in Lake Uru Uru sediments than in the Cala Cala Lagoon with a lower contribution of the residual fraction (R) and a higher contribution of the exchangeable fraction (F1) for Lake Uru Uru (Figs. 3 and 4; Table 4). Solid state partitioning profiles in Lake Uru Uru show differences between the northern and southern areas (Fig. 4). The main differences include: (i) higher extractability of Cd in the northern part of the lake, with a lower mean contribution of the residual fraction (R; ca. 13%) and a higher mean contribution of the exchangeable fraction (F1; ca. 50%) compared to the southern part of the lake (ca. 26% for R and ca. 36 for F1); (ii) higher extractability of As in the northern part, while U is more reactive in the southern part; (iii) higher mean contribution of the reducible fraction (F3) for Mn in the northern part (ca. 50%) than in the southern part (ca. 27%).

The differences in the solid state partitioning between the northern and the southern part of Lake Uru Uru are for the most part input-related differences: sediments of the northern part of the lake are fed by particles from the Thajarita River and Tagarete Channel, that drain wastes from the San José mine (Ag–Pb–Zn–Au) while being fed by particles from the Desaguadero River and the San Juan de Sora Sora River, that drains wastes from the Huanuni mine (Sn) in the southern part of the lake. Additionally, the differences in the solid state partitioning between the northern and the southern part of Lake Uru Uru can be explained by the fact that (i) the northern part is periodically subjected to desiccation due to shallowness and (ii) the southern part is characterized by a higher density of aquatic vegetation (see Section 2.2). This most likely triggers differences in geochemical processes at the water–sediment interface and, therefore, in the solid state partitioning between the two parts of the lake. Solid state partitioning shows fairly coherent patterns between dry and wet seasons. However some differences can be noted. In Northern Lake Uru Uru sediments, operationally-defined reactive fractions extracted from DS exhibit slightly lower average contributions to the TMC than in WS (Fig. 4a and b). Overall, the operationally-defined reactivity (mobility) of the trace elements and metalloids in this part of the lake is as follows: Fe < Zn < Cu < U < Pb < Sb < As < Cd < Mn. In Southern Lake Uru Uru, the operationally-defined reactivity ranking of trace metals and metalloids is similar to that of the northern part. The only marked discrepancies are for As and U, with a significantly higher contribution of fraction F3 in the dry season. These differences between the dry and wet seasons can be assigned to spatial heterogeneity rather than heterogeneity of geochemical

Table 3
Total particulate concentrations (mg kg^{-1}) of trace metals and metalloids in the sampled sediment cores, and mean enrichment factors (EFs) related to the Upper continental crust (UCC) composition from Wedepohl (1995) and our local reference site Cala Cala Lagoon (CCLAC). Titanium was used as a conservative element for normalization. DS, dry season; WS, wet season.

		Mn	Fe	Cu	Zn	Cd	Pb	U	As	Sb
UCC		527	30,890	25	52	0.1	14.8	1.7	1.7	2.3
Cala Cala Lagoon	Mean	657	38,707	49	121	0.5	107	4.3	51	12
	Median	636	38,080	49	119	0.4	109	4.1	51	12
	Min–Max	572–833	34,430–47,840	39–66	104–147	0.3–1.1	61–149	3.1–5.7	38–72	3.1–5.7
	2σ	68	3300	7	10	0.2	24	0.8	8	2
	EF_{UCC}	1	1	2	1	3	4	1	14	22
North. Uru Uru DS	Mean	654	28,700	65	152	1.6	48	2.9	62	16
	Median	656	28,135	69	157	1.6	45	2.9	62	15
	Min–Max	508–743	23,850–34,770	43–81	107–183	1.1–2.0	38–60	2.5–3.5	49–76	2.5–3.5
	2σ	73	2550	13	22	0.3	6	0.3	7	3
	EF_{UCC}	1	1	4	3	14	3	1	28	45
	EF_{CCLAC}	2	1	2	2	5	1	1	2	2
North. Uru Uru WS	Mean	547	34,840	57	127	1.3	41	2.3	49	13
	Median	543	34,530	58	127	1.4	40	2.4	47	14
	Min–Max	481–591	32,380–38,440	49–63	109–138	0.6–1.7	33–50	1.8–2.8	37–60	1.8–2.8
	2σ	31	1700	4	8	0.3	4	0.3	7	4
	EF_{UCC}	1	1	4	2	12	2	1	23	39
	EF_{CCLAC}	1	1	2	2	4	1	1	2	2
South. Uru Uru DS	Mean	531	28,530	82	133	0.5	51	3.7	70	9
	Median	519	28,070	85	136	0.5	43	3.3	66	7
	Min–Max	381–650	22,780–35,770	38–115	101–167	0.3–0.9	33–100	2.1–5.3	47–103	2.1–5.3
	2σ	77	2771	16	17	0.1	17	1	16	4
	EF_{UCC}	1	1	6	3	5	3	2	37	31
	EF_{CCLAC}	2	1	3	2	2	1	2	3	1
South. Uru Uru WS	Mean	411	28,420	73	116	0.7	67	2.9	63	12
	Median	375	30,860	78	108	0.6	36	2.6	61	7
	Min–Max	298–647	10,180–36,700	28–103	43–222	0.3–1.3	13–163	1.9–5.4	30–104	1.9–5.4
	2σ	126	7290	20	40	0.3	52	1	19	10
	EF_{UCC}	1	1	7	3	9	5	2	43	46
	EF_{CCLAC}	2	2	4	2	3	1	2	3	2

Table 4
Mean metal concentrations (mg kg^{-1}) in the operationally-defined fractions extracted from the five studied sediment cores. F1: exchangeable; F2: carbonates; F3: Fe- and Mn-oxyhydroxides; F4: sulfides and/or organic matter. DS, dry season; WS, wet season.

	Cala Cala Lagoon	North. Uru Uru DS	North. Uru Uru WS	South. Uru Uru DS	South. Uru Uru WS
Manganese (mg kg^{-1})					
F1	89.3	23.7	20.5	56.7	52.0
F2	137	209	218	192	258
F3	312	312	289	151	106
F4	470	72.8	81.3	79.1	47.4
Iron (mg kg^{-1})					
F1	0.63	0.26	<d.l.	0.14	0.26
F2	1143	240	811	499	1387
F3	3117	1461	1908	4476	3766
F4	0.2	<d.l.	<d.l.	1.2	0.25
Copper (mg kg^{-1})					
F1	0.05	0.76	0.33	1.3	0.35
F2	2.3	11.2	13.7	15.7	18.3
F3	1.1	0.75	0.27	0.47	0.40
F4	1.1	3.7	2.9	4.9	5.8
Zinc (mg kg^{-1})					
F1	3.1	3.6	2.0	2.4	1.6
F2	3.3	7.1	11.7	15.7	13.0
F3	7.4	14.6	14.0	11.9	11.9
F4	0.89	0.12	0.17	0.95	0.39
Cadmium (mg kg^{-1})					
F1	0.18	0.85	0.57	0.23	0.15
F2	0.03	0.37	0.38	0.11	0.20
F3	0.05	0.12	0.07	<d.l.	<d.l.
F4	0.07	0.15	0.16	0.12	0.05
Lead (mg kg^{-1})					
F1	0.16	0.06	0.05	0.05	0.08
F2	9.1	12.1	13.5	10.1	30.8
F3	5.9	5.8	5.5	3.4	10.7
F4	0.03	0.01	0.01	0.02	0.03
Uranium (mg kg^{-1})					
F1	<d.l.	0.09	0.11	0.19	0.42
F2	0.84	0.39	0.28	1.0	1.3
F3	0.94	0.42	0.28	1.2	1.6
F4	0.12	0.07	0.04	0.21	0.26
R					
Arsenic (mg kg^{-1})					
F1	0.09	1.0	0.46	0.39	0.18
F2	5.2	12.4	11.8	7.4	10.8
F3	22.3	34.2	35.3	42.6	37.9
F4	0.07	1.5	0.88	0.41	0.43
Antimony (mg kg^{-1})					
F1	0.22	0.33	0.71	0.23	0.63
F2	0.53	1.4	1.5	0.61	1.2
F3	2.0	4.2	4.8	3.3	4.4
F4	0.23	0.87	0.91	0.19	0.57

processes occurring within the sediments. However, the first centimeters below the water–sediment interface reveal marked differences between the wet and dry seasons (Fig. 4). The solid state partitioning in the very first centimeters below the water–sediment interface is strongly affected by redox reactions driven by early diagenesis processes (see Section 4). The latter are themselves controlled by environmental conditions (such as temperature, O_2, and particulate organic C concentration) that are contrasted between the dry and wet seasons.

3.2. Dissolved phase

3.2.1. Chloride, sulfate and N-species

Porewater from the Cala Cala Lagoon exhibits a concave-shaped Cl^- profile (Fig. 5a) with concentrations sharply decreasing within the first 20 cm below the WSI from 0.59 to 0.22 mM and then increasing to reach 0.82 mM at the bottom of the core. Porewater SO_4^{2-} concentrations decrease sharply in the first 5 cm of sediments from 0.32 mM in the BW to concentrations below the DL, indicating dissolved SO_4^{2-} consumption just below the WSI. Accordingly, diffusive fluxes indicate that the Cala Cala Lagoon sediments represent an important sink of dissolved SO_4^{2-} (9.41 μmol cm^{-2} a^{-1}; Table 5) for the overlying WC. Nitrate concentrations range from 1.0 to 5.6 μM and show a very scattered pattern with depth (Fig. 5a). Ammonium in porewater shows overall increasing concentrations with depth from 0.2 mM in the BW to 1.0 mM at the bottom of the core (Fig. 5a).

In Lake Uru Uru, Cl^- depth profiles show concentrations increasing almost linearly in DS for both the northern and southern parts (Fig. 5b and c). In WS, the southern part is also characterized by increasing Cl^- concentrations with depth while the northern part shows nearly constant concentrations (14.9 ± 2.3 mM). All dissolved SO_4^{2-} concentration–depth profiles mimic those of Cl^- (R^2 = 0.78; Fig. 5b and c; Table 6). Similarly to the Cala Cala Lagoon, the NO_3^- concentration–depth profiles exhibit strong data scattering, particularly for WS. Nitrate concentrations in DS tend to

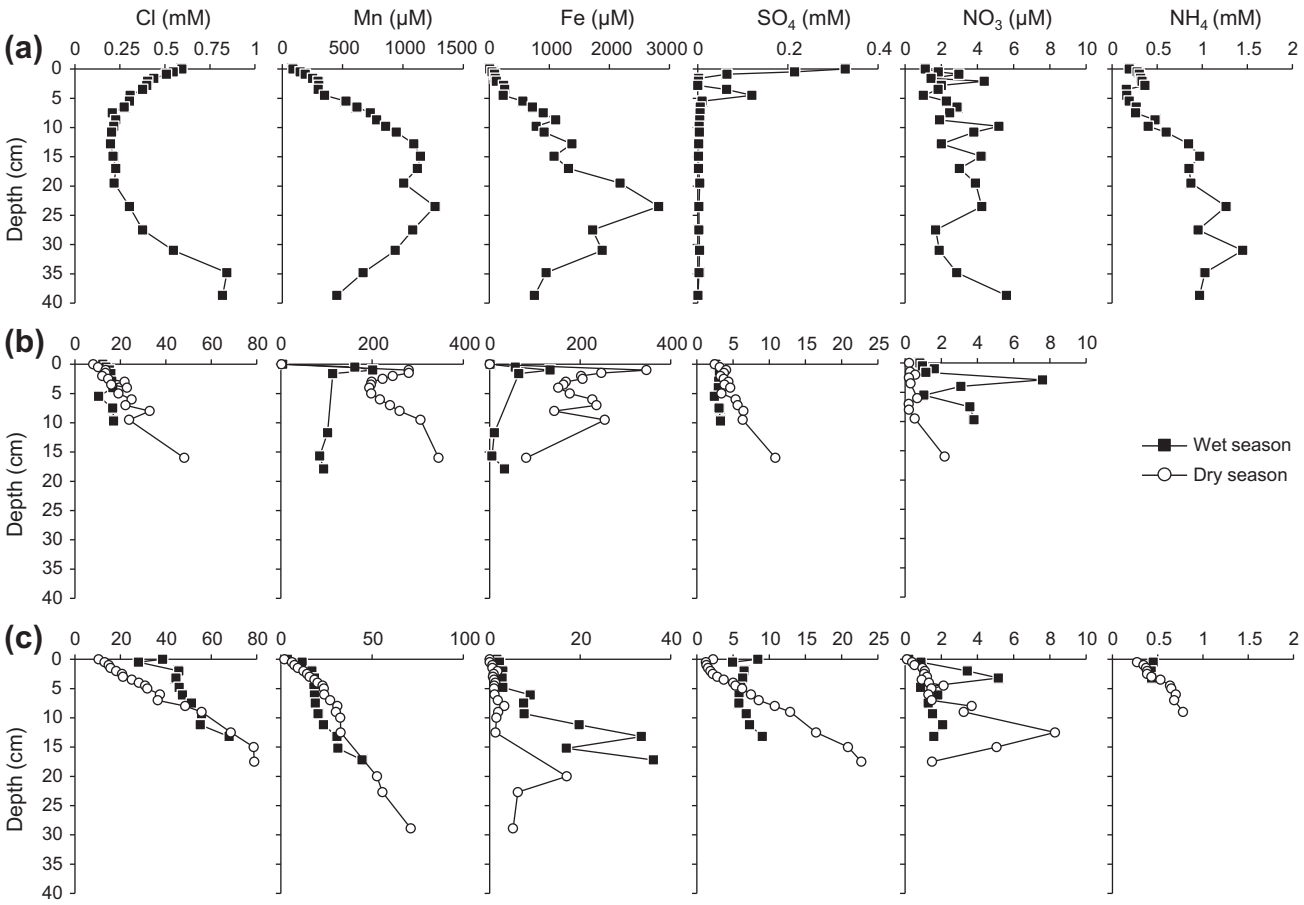

Fig. 5. Concentration–depth profiles for Cl^-, Fe, Mn, SO_4^{2-} and N-species in the porewater of the Cala Cala Lagoon (a), Northern (b) and Southern (c) Lake Uru Uru. Bottom water (BW) composition is reported at depth = 0. Note scale differences for concentrations from site to site.

increase gently with depth (from 0.2 to 2.2 μM) in the northern part of the lake while strongly increasing (up to 8.2 μM) in the southern part (Fig. 5b and c). Ammonium concentrations (only determined in the southern cores) increase steadily (from 0.3 to 0.8 mM) with depth for DS. In contrast, in WS, NH_4^+ concentrations stay constant (~0.45 mM) in the first 4 cm below the WSI (Fig. 5c).

3.2.2. Dissolved Fe and Mn

In the Cala Cala Lagoon, dissolved Fe and Mn concentrations are low (9 and 89 μM, respectively) in the BW (Fig. 5a). In the sediment, porewater Fe and Mn show fairly similar convex-shaped profiles, both depicting first increasing concentrations (up to 2820 and 1270 μM, respectively) in the first 23 cm below the WSI, indicating production of both elements at this depth, and decreasing concentrations (consumption) deeper in the sediment. Accordingly, diffuse transport indicates efflux of Fe and Mn (5.18 and 3.11 μmol cm^{-2} a^{-1}, respectively; Table 5) at the water–sediment interface.

The northern and southern parts of Lake Uru Uru exhibit contrasting porewater Fe and Mn profiles (Fig. 5b and c) and very low concentrations in BW (<2 and <5 μM, respectively). In the northern part, production of dissolved Fe and Mn is evidenced by increasing concentrations of both elements (up to 346 and 281 μM, respectively) just below the WSI for both WS and DS (Fig. 5b). Decreasing concentrations of porewater Fe and Mn, implying removal, are observed below the first cm of sediment for both WS and DS. Significant (DS) and near-total (WS) Fe removal is observed below 10 cm depth. In contrast, Mn concentrations below the decreasing zone stay constant (94 ± 9 μM; WS) or even increase (up to 346 μM; DS). In the southern part, porewater Fe and Mn are characterized by contrasting concentration-depth profiles (Fig. 5c). For both DS and WS, steadily increasing dissolved Mn concentrations are observed suggesting that the dissolved Mn production zone is situated deeper than the bottom of the core. Porewater Fe concentrations stay close to detection limit in the first 5 (WS) and 13 (DS) cm below the WSI and then increase quite sharply (e.g., up to 38 μM; WS). Porewater Fe removal is observed below 20 cm depth for DS. In general, sediments from Lake Uru Uru are a potential source of dissolved Fe and Mn to the overlying WC (Table 5).

3.2.3. Dissolved trace metals and metalloids

Trace metals and metalloids in porewater show variable profiles between the Cala Cala Lagoon and Lake Uru Uru and between both seasons. In the former, As, Sb, Pb and U show positive concentration gradients just below the WSI (Fig. 6a). In contrast, Cu, Zn and Cd porewater profiles are characterized by decreasing concentrations just below the WSI. Well-resolved concentration peaks at ~5–7 cm depth for U and Sb identify a production zone for both elements. The Cala Cala Lagoon sediments are a source of dissolved As, Sb, Pb and U for the overlying WC (e.g., up to 0.63 μmol cm^{-2} a^{-1} for As; Table 5) while being a sink of Cu, Zn and Cd (e.g., 7.23×10^{-3} μmol cm^{-2} a^{-1} for Cu).

The northern part of Lake Uru Uru in DS shows porewater concentrations below DL within the first 2.5 cm below the WSI for all the trace metals and metalloids (Fig. 6b). Below this depth, increasing concentrations are observed as a general trend, with the presence of peaks at ~6 cm depth for Cd (0.2 nM) and Pb (2.1 nM). The

Table 5
Diffusive transport through the water–sediment interface in the Cala Cala Lagoon and Lake Uru Uru.

	NO_3	SO_4	Fe	Mn	Zn	Cd	Pb	Cu	As	Sb	U
Cala Cala Lagoon											
Dsed ($cm^2\ s^{-1}$)	8.84E−06	4.82E−06	3.20E−06	3.17E−06	3.22E−06	3.22E−06	4.28E−06	3.32E−06	4.13E−06	3.76E−06	1.95E−06
$\partial C/\partial z$ ($\mu mol\ cm^{-4}$)	−2.06E−03	2.03E−01	−1.69E−01	−1.02E−01	4.58E−04	1.57E−07	−3.38E−06	2.28E−04	−1.58E−02	−2.53E−05	−9.41E−05
Jsed ($\mu mol\ cm^{-2}\ s^{-1}$)[a]	1.33E−08	−7.16E−07	3.95E−07	2.37E−07	−1.08E−09	−3.69E−13	1.06E−11	−5.52E−10	4.77E−08	6.96E−11	1.34E−10
Jsed ($\mu mol\ cm^{-2}\ yr^{-1}$)[b]	1.74E−01	−9.41E+00	5.18E+00	3.11E+00	−1.41E−02	−4.84E−06	1.39E−04	−7.25E−03	6.26E−01	9.14E−04	1.76E−03
North. Uru Uru DS											
Dsed ($cm^2\ s^{-1}$)	8.13E−06	4.44E−06	2.95E−06	2.92E−06	2.96E−06	2.96E−06	3.94E−06	3.05E−06	3.80E−06	3.46E−06	1.79E−06
$\partial C/\partial z$ ($\mu mol\ cm^{-4}$)	−7.55E−05	−5.24E−01	−3.46E−01	−2.79E−01	–	–	–	–	−7.02E−03	–	3.89E−06
Jsed ($\mu mol\ cm^{-2}\ s^{-1}$)[a]	4.18E−10	1.58E−06	6.94E−07	5.54E−07	–	–	–	–	1.81E−08	–	−4.73E−12
North. Uru Uru WS											
Dsed ($cm^2\ s^{-1}$)	1.03E−05	5.63E−06	3.74E−06	3.70E−06	3.75E−06	3.76E−06	5.00E−06	3.87E−06	4.82E−06	4.39E−06	2.27E−06
$\partial C/\partial z$ ($\mu mol\ cm^{-4}$)	−2.34E−03	−2.91E−01	−1.33E−01	−1.97E−01	−6.93E−05	−1.26E−07	−3.02E−06	7.12E−05	−7.50E−03	1.70E−05	1.99E−05
Jsed ($\mu mol\ cm^{-2}\ s^{-1}$)[a]	1.97E−08	1.34E−06	4.07E−07	5.98E−07	2.13E−10	3.88E−13	1.24E−11	−2.26E−10	2.96E−08	−6.13E−11	−3.70E−11
North. Uru Uru											
Jsed ($\mu mol\ cm^{-2}\ yr^{-1}$)[b]	1.32E−01	1.92E+01	7.23E+00	7.57E+00	1.40E−03	2.55E−06	8.13E−05	−1.49E−03	3.14E−01	−4.03E−04	−2.74E−04
South. Uru Uru DS											
Dsed ($cm^2\ s^{-1}$)	1.26E−05	6.86E−06	4.56E−06	4.51E−06	4.58E−06	4.58E−06	6.10E−06	4.72E−06	5.88E−06	5.35E−06	2.77E−06
$\partial C/\partial z$ ($\mu mol\ cm^{-4}$)	−1.95E−04	5.72E−02	−1.02E−04	−2.40E−03	−1.50E−05	−5.32E−08	−1.01E−07	−1.31E−06	−3.16E−03	−5.15E−05	−2.35E−06
Jsed ($\mu mol\ cm^{-2}\ s^{-1}$)[a]	2.28E−09	−3.65E−07	4.33E−10	1.01E−08	6.39E−11	2.27E−13	5.71E−13	5.76E−12	1.73E−08	2.56E−10	6.06E−12
South. Uru Uru WS											
Dsed ($cm^2\ s^{-1}$)	1.05E−05	5.73E−06	3.80E−06	3.77E−06	3.82E−06	3.82E−06	5.09E−06	3.94E−06	4.90E−06	4.47E−06	2.31E−06
$\partial C/\partial z$ ($\mu mol\ cm^{-4}$)	−1.55E−03	6.94E+00	−2.74E−04	−6.72E−03	2.49E805	−3.08E−07	1.98E−06	1.28E−05	−2.35E−02	−9.45E−04	−5.26E−05
Jsed ($\mu mol\ cm^{-2}\ s^{-1}$)[a]	1.35E−08	−3.30E−05	8.64E−10	2.10E−08	−7.88E−11	9.76E−13	−8.35E−12	−4.18E−11	9.56E−08	3.50E−09	1.01E−10
South. Uru Uru											
Jsed ($\mu mol\ cm^{-2}\ yr^{-1}$)[b]	1.04E−01	−2.19E+02	8.52E−03	2.04E−01	−9.77E−05	7.90E−06	−5.11E−05	−2.36E−04	7.41E−01	2.47E−02	7.02E−04

[a] Diffusive fluxes were calculated using Fick's first law: $Jsed = -\varnothing Dsed(\partial C/\partial z)$, where *Dsed* is the diffusion coefficient corrected for temperature and tortuosity, $\varnothing$ is porosity assuming an average sediment density of 2.65 g cm^3 and measured water content, and $\partial C/\partial z$ is the linear concentration gradient across the water–sediment interface. Positive *Jsed* indicates an upward-directed flux (efflux from the sediment into the overlying water column) and negative *Jsed* indicates a downward-directed flux (influx from the water column into the sediment).

[b] Annual rates of diffusive transport for the Cala Cala Lagoon were integrated over 365 days and as the integrated average over both seasons for Lake Uru Uru.

Table 6
Determination coefficient (R^2) for linear regression between porewater chloride and sulfate and porewater trace metals and metalloids in the Cala Cala Lagoon and Lake Uru Uru sediments. DS, dry season; WS, wet season. $R^2 \geqslant 0.7$ in bold.

		Mn	Fe	Cu	Zn	As	Cd	Sb	Pb	U
Cala Cala Lagoon	Cl^-	0.24	0.07	0.11	0.04	0.25	0.19	0.38	0.10	0.05
	SO_4^{2-}	0.33	0.21	0.50	0.00	0.11	0.02	0.07	0.00	0.01
North. Uru Uru DS	Cl^-	0.32	0.42	**0.73**	**0.89**	0.10	0.62	**0.89**	0.56	**0.74**
	SO_4^{2-}	0.42	0.23	**0.71**	**0.88**	0.08	0.48	**0.83**	0.53	**0.74**
North. Uru Uru WS	Cl^-	0.43	0.55	**0.85**	0.16	**0.77**	0.65	**0.87**	0.01	0.68
	SO_4^{2-}	0.58	0.63	**0.94**	0.30	**0.86**	0.51	**0.96**	0.03	**0.82**
South. Uru Uru DS	Cl^-	**0.86**	0.40	**0.75**	**0.78**	0.39	**0.84**	**0.72**	**0.71**	**0.79**
	SO_4^{2-}	**0.80**	0.37	**0.71**	**0.72**	0.40	**0.85**	**0.70**	0.67	**0.79**
South. Uru Uru WS	Cl^-	**0.72**	0.67	0.24	0.02	0.03	0.04	0.01	0.03	0.17
	SO_4^{2-}	0.06	0.39	0.15	0.01	0.59	0.19	0.42	0.01	0.01

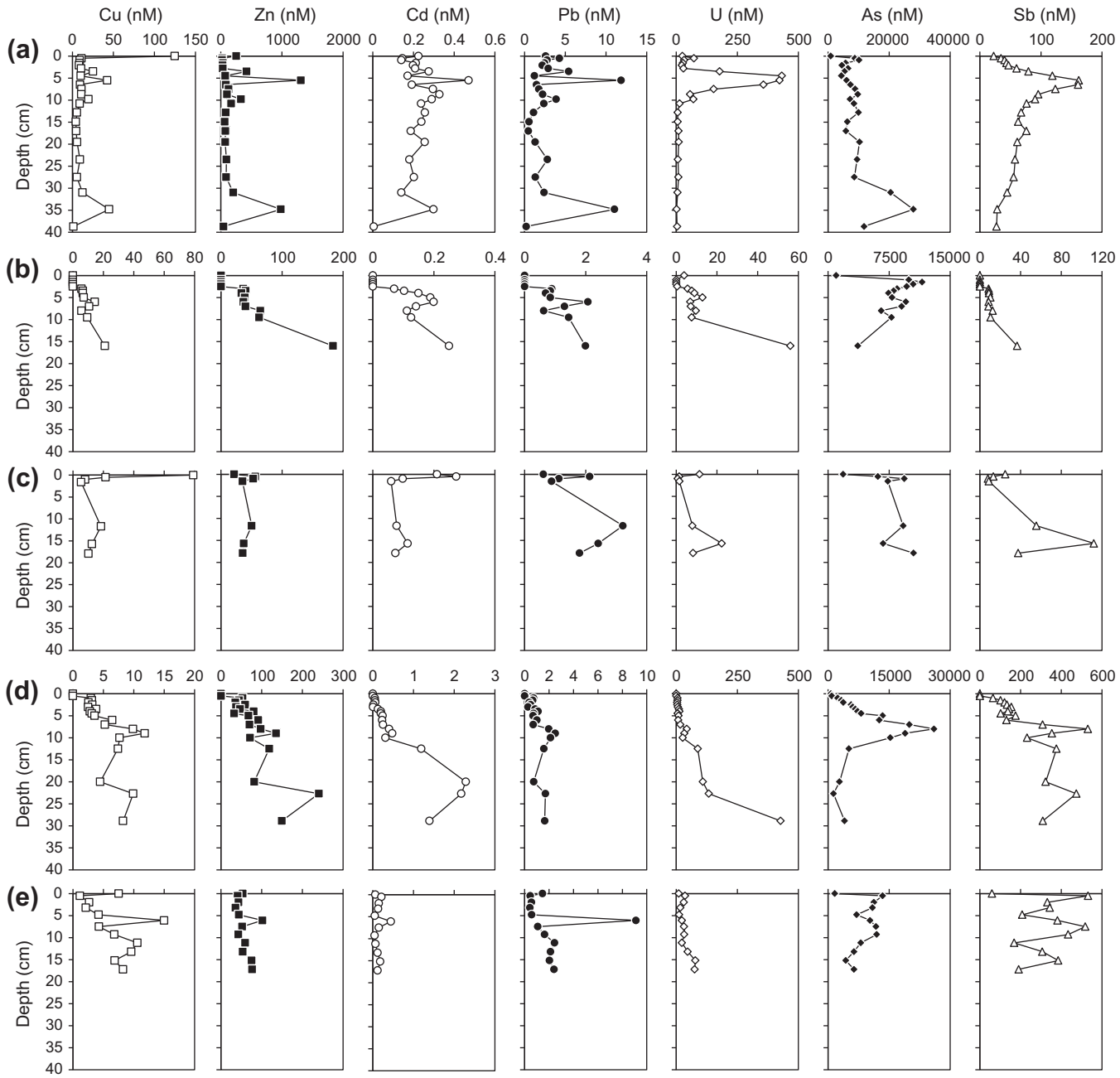

Fig. 6. Concentration–depth profiles of trace metals and metalloids in the porewater of the Cala Cala Lagoon (a), Northern Lake Uru Uru in dry (b) and wet (c) seasons and Southern Lake Uru Uru in dry (d) and wet (e) seasons. Bottom water (BW) composition is reported at depth = 0.

porewater As distribution contrasts with those of the other trace metals and metalloids, mimicking that of porewater Fe (Fig. 5b). In WS, trace metals and metalloids can be split into two groups (Fig. 6c): (i) Cu, Sb and U with porewater profiles characterized by negative concentration gradients just below the WSI, and in contrast (ii) Zn, As, Cd and Pb showing positive concentration gradients just below the WSI. Deeper in the sediment, either increasing concentrations with depth (Sb and Pb) or flat profiles (i.e., constant concentrations; Cu, Zn, As and Cd) are observed. Additionally, removal of Sb, Pb and U to a lesser extent is observed at the bottom of the core.

The southern part of Lake Uru Uru for DS is characterized by porewater concentrations below detection limit for Cd, Pb and U within the first centimeter depth below the WSI (Fig. 6d). Below this depth, porewater concentrations of these trace metals show either concave-shaped profiles (Cd), or increasing (U) or nearly constant (Pb) patterns. Porewater Cu, Zn, As and Sb show positive concentration profiles in the first 10 cm below the WSI with, for instance, As concentrations reaching up to 26,000 nM at 8 cm depth (Fig. 6d). Deeper, these trace metals and metalloids show contrasting behaviors as they are either almost totally removed from porewater (As) or show increasing concentrations. In WS, trace metal and metalloid porewater profiles show fewer variations than those in DS (Fig. 6e). Zinc and Cd show quite flat profiles with concentrations centered on 57 and 0.14 nM, respectively. Copper and Pb profiles exhibit negative concentration gradients through the WSI and a well-resolved peak (15 and 9 nM, respectively) at 6 cm depth and then increasing concentrations. According to diffusive transport (Table 5), Lake Uru Uru sediments are always a source of dissolved Cd and As for the overlying WC (e.g., up to 0.74 μmol cm^{-2} a^{-1} for As, southern part) and a sink of dissolved Cu (with rates up to 1.49×10^{-3} μmol cm^{-2} a^{-1} in the northern part). For the other trace metals and metalloids, the sediments are either a sink or a source depending on the season and/or location.

4. Discussion

4.1. Early diagenesis processes and organic matter mineralization pathways

Redox processes accompanying OM mineralization, i.e. early diagenesis (Berner, 1980), are expected to control the fate of the metal-bearing phases present in the sediment pile. Depth distribution of major dissolved redox species (Mn, Fe, SO_4^{2-}, N-species) is characterized by concentration gradients just below the WSI driven by the bacterially-mediated oxidation of OM (Froelich et al., 1979; Postma and Jakobsen, 1996). These processes are discussed in the following.

4.1.1. The Cala Cala Lagoon

In the sediments of the Cala Cala Lagoon, OM mineralization proceeds mainly through anaerobic reactions. Dissimilatory (bacteria-mediated) SO_4 reduction and reductive dissolution of Mn- and Fe-oxyhydroxides are evidenced by sharply decreasing dissolved SO_4^{2-} concentrations and increasing dissolved Fe and Mn concentrations below the WSI and associated NH_4^+ production (Fig. 5a). Reductive dissolution of Mn- and Fe-oxyhydroxides is further supported by the overall decrease of the contribution of Fe_{asc} (from 11% to 4%) and Mn_{asc} (from 60% to 24%) from just below the water–sediment interface to 17-cm depth (Fig. 5). As a result of reductive dissolution of Fe-oxyhydroxides, upward-directed diffusive transport of Fe and Mn through the WSI is evidenced (Table 5). However, no accumulation of dissolved Fe and Mn is observed in the overlying BW (Fig. 5a). This may be explained by the existence of a redox loop related to the oxygenated BW promoting oxidative precipitation of Mn and Fe diffusing through the WSI from the sediment and, therefore, concentrating Fe- and Mn-oxyhydroxides in surface sediments (Davison, 1993; Boudreau, 1999). This is supported, for example, by the steep increase of the Mn_{asc} contribution from 4.2% at the water–sediment interface to 60% at 1-cm depth. Slight enrichment of SO_4^{2-} (up to 0.12 mM at 4.5 cm depth) is observed (Fig. 5a). This excess of dissolved SO_4^{2-} is likely to be attributable to bacterial production of SO_4^{2-} from dissolved reduced sulfides, that had not reacted with dissolved reduced Fe, and is coupled with NO_3^- reduction (Suits and Arthur, 2000) as the observed excess of dissolved SO_4^{2-} occurs at a depth where NO_3^- is present in porewater. Additional production of SO_4^{2-} could be provided by chemical re-oxidation of dissolved sulfide by Fe- and Mn- oxyhydroxides (Aller and Rude, 1988; Böttcher and Thamdrup, 2001) and/or by O_2 in oxygenated micro-environments likely present in the sediment. Under the change of pH associated with early diagenetic processes (Boudreau, 1997), diagenetically-reduced Fe and Mn present as Fe- and Mn-rich carbonates likely also contributes to porewater Fe and Mn. This contention is supported by significant Fe and Mn extracted by NaOAc (fraction F2; Table 4). Below the active layer of reductive dissolution (25 cm depth), dissolved Fe and Mn are removed from porewater (Fig. 5a) most likely due to precipitation of authigenic phases. Manganese is likely mainly associated with carbonates as suggested by the increase of the contribution of fraction F2 (from 19% to 41%) between 27 and 35 cm depth (Fig. 3). In contrast, Fe is mainly incorporated in authigenic sulfides, as supported by the increase of fraction F3 from 6% to 13% below 25 cm depth (Fig. 3), as well as being adsorbed on inorganic or organic particulates as reported for other freshwater environments (Davison, 1993; Audry et al., 2010). However, the formation of non-sulfidic authigenic minerals such as Fe-carbonates (Aller et al., 2004) could represent an additional, albeit minor (Fe_{NaOAc} = 3.7 ± 1.1% below 23 cm depth), control on Fe solubility at depth.

Bacterial denitrification, another pathway for OM mineralization in anaerobic sediments (Froelich et al., 1979), is not evidenced in those sediments since no NO_3^- decrease is observed below the WSI (Fig. 5a). On the contrary, an overall increase of NO_3^- is observed from the BW (1.13 μM) to the bottom of the core (5.6 μM), suggesting that NO_3^- is produced (anoxic nitrification), likely through the reduction of Mn-oxyhydroxides by NH_4^+ (Hulth et al., 1999; Hyacinthe et al., 2001). It is, therefore, possible that little denitrification actually proceeds in the first centimeters of the sediment while being masked by higher rates of anoxic nitrification. Therefore, OM mineralization in the Cala Cala Lagoon sediment is likely mainly supported by dissimilatory reduction of SO_4 and Fe- and Mn-oxyhydroxides.

4.1.2. Lake Uru Uru

In addition to the OM present in the sediment, early diagenetic processes in Lake Uru Uru are fuelled by OM inputs at the WSI from primary production in the WC and allochtonous OM from rivers. The higher POC content observed in the sediment top layers of Southern Lake Uru Uru compared to the northern part (Fig. 2b–e) can be attributed to permanent OM input into the sediment, due to the perennial presence of the WC and the associated primary production. In contrast, in the northern part of the lake, the seasonal disappearance of the WC decreases the annual OM inputs into the sediments.

Assessment of early diagenetic processes and OM mineralization pathways from porewater concentration-depth profiles can be hindered by evaporation- and input-related processes. For both the northern and southern parts of Lake Uru Uru, DS is characterized by linearly and sharply increasing porewater Cl^- and SO_4^{2-} with depth (Fig. 5b and c) with correlated concentrations ($R^2 > 0.87$). These patterns are likely related to both high evaporation rates

during the dry season (UNEP, 1996) and high inputs of Cl^- and SO_4^{2-} at the WSI. High inputs of Cl^- and SO_4^{2-} likely originate from the alteration of gypsum, anhydrite and halite that are important constituents of the Altiplano Salars (e.g., Salar de Coipasa and Salar de Uyuni; (Risacher and Fritz, 1991), and of alunite which is one of the major constituents of the alteration zones surrounding the Sb

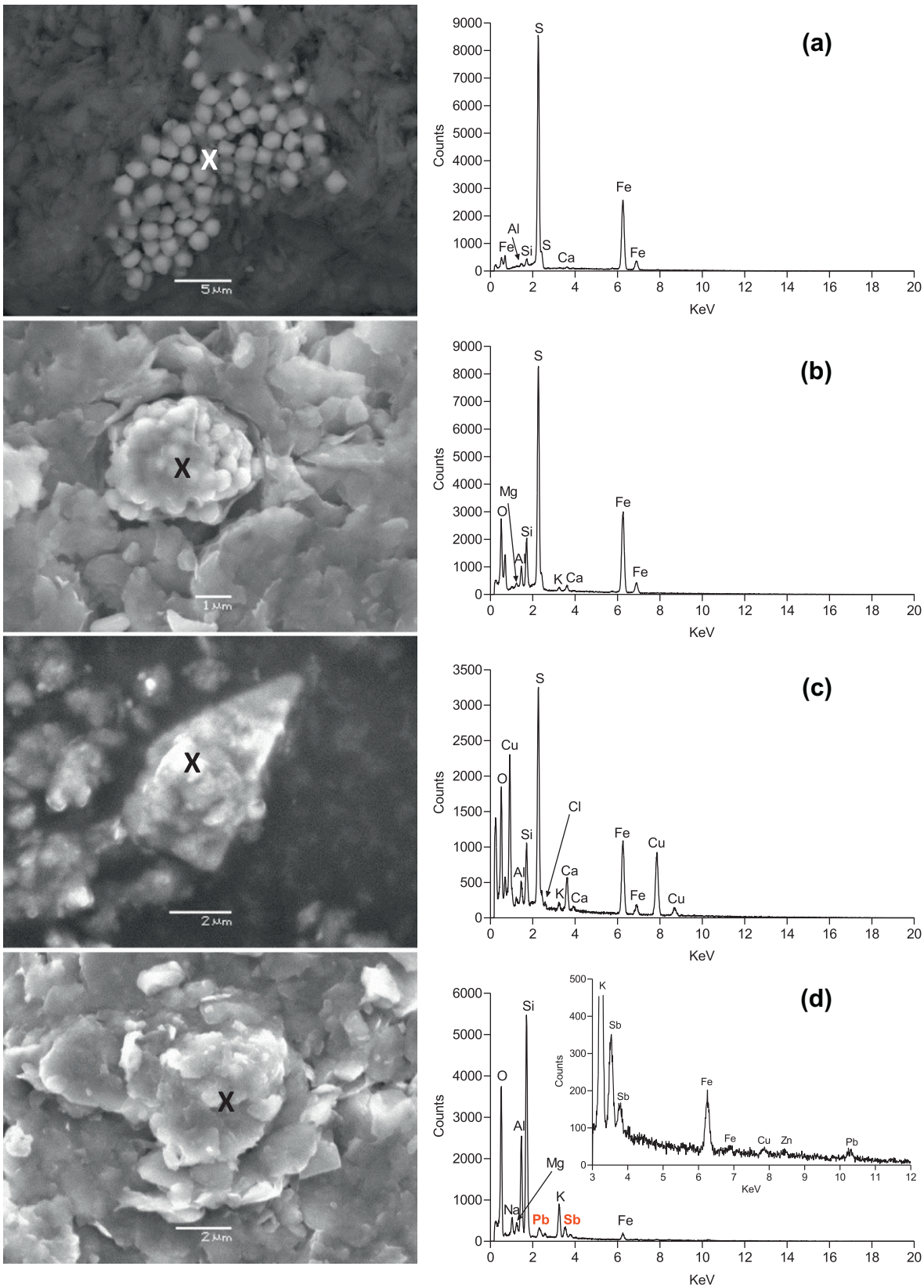

Fig. 7. SEM photomicrographs and associated EDS patterns of selected trace element-bearing particles from Northern (a) and Southern (b–d) Lake Uru Uru sediments. Authigenic (a) and framboidal (b) Fe sulfides containing As (up to 0.2 wt.% as revealed by electron microprobe analysis); (c) chalcopyrite embedded in a silicate matrix; (d) silicate particle containing trace metals (Cu, Zn, Pb) and metalloid (Sb). The 'X' indicates the EDS spot.

mineralization in the Tertiary volcanites of the Bolivian Andes (Dill, 1998). As a consequence, SO_4 reduction cannot be clearly evidenced in Northern Lake Uru Uru during both seasons (Fig. 5b). However, decreasing Cl-normalized SO_4^{2-} concentrations (not shown) just below the WSI in both the northern and southern parts of Lake Uru Uru suggest that SO_4 reduction is actually proceeding in these sediments.

Another mineralization pathway for OM in Lake Uru Uru sediments is the dissimilatory reduction of Fe- and Mn-oxyhydroxides, as evidenced by increasing porewater Fe and Mn concentrations with depth (Fig. 5b and c). In the northern part of the lake, the sharp porewater Fe and Mn concentration gradients just below the WSI in both seasons (Fig. 5b) suggest the rapid and shallow onset of dissimilatory reduction processes following the re-instalment of a WC after seasonal dry periods. The vertical distribution of Fe and Mn in the ascorbate fraction (F3; Fig. 4a and b) suggests that reoxidation of reduced porewater Fe and Mn in the sediment can be a significant process during periods when this part of the lake is dry. A second zone of Fe and Mn reductive dissolution is evidenced deeper in the sediment (10 cm depth; Fig. 5b) in DS, likely involving less reactive Fe- and Mn-oxyhydroxides. In the southern part of the lake (not experiencing complete seasonal desiccation), the production of porewater Fe and Mn through dissimilatory reduction of Fe- and Mn-oxyhydroxides proceeds deeper in the sediment (>10 cm depth for Fe and deeper than the maximum sampling depth for Mn; Fig. 5c). This is supported by the overall decrease with depth of Fe and Mn extracted by ascorbate for both seasons (Fig. 4c and d). In addition, aging (less and less amorphous) through time and burial of the Fe- and Mn-oxyhydroxides precipitated at the WSI could also contribute to the observed decrease of fraction F3 with depth. Despite the upward-directed diffusive transport of dissolved Fe and Mn (Table 5) generated by the concentration gradients built up by dissimilatory reduction of Fe- and Mn-oxyhydroxides, these two elements do not accumulate above the WSI (Fig. 5b and c). The so-called redox loop, which concentrates newly precipitated Fe- and Mn-oxyhydroxides in near-surface sediments (Davison, 1993; Boudreau, 1999), is likely responsible for the very low (close to detection limit) dissolved Fe and Mn concentrations observed in the bottom water. The accumulation of newly precipitated Fe- and Mn-oxyhydroxides near the WSI is supported by the occurrence of peaks of fraction F3 for Fe and Mn just below the WSI (Fig. 4d). A consequence of the redox loop is the partial regeneration of the Fe- and Mn-oxyhydroxides pool involved in the OM mineralization processes. In contrast, in Southern Lake Uru Uru, Fe released into porewater by dissimilatory reduction does not diffuse to the WC, as shown by the flat profiles below the WSI (Fig. 5c). These profiles indicate that a pumping process is removing Fe from the porewater before it reaches the WSI by diffusion. This could be explained by biological uptake of dissolved Fe by aquatic plants which density is high in Southern Lake Uru Uru (see Section 2.2). It has been reported that the three main plant species present in Southern Lake Uru Uru (*Totora*, *Ruppia* and *Chara*) are characterized by high capacity to uptake Fe from porewater and concentrate this metal in their tissues (Gehler, 1984; Kufel and Kufel, 2002; Malea et al., 2008). The intense biological Fe uptake results in a weakening of the redox loop. This likely promotes the exhaustion of Fe-oxyhydroxides (electron acceptors) available for reduction over time and, therefore, less effective OM mineralization.

The total (northern part, WS; Fig. 5b) or partial (northern and southern parts, DS; Fig. 5b and c) removal of Fe from porewater at depth points towards precipitation of authigenic Fe minerals and adsorption on inorganic and/or organic particulates as reported for other freshwater environments (e.g. Davison, 1993; Audry et al., 2010). Framboidal and poorly-crystalline Fe-sulfides were observed both in the northern (Fig. 7a) and southern (Fig. 7b) parts of Lake Uru Uru, indicating that authigenic sulfide minerals partly control the Fe solubility at depth in the sediments. However, a low contribution of the oxidizable fraction (F4) in Fe partitioning is observed for all cores (Fig. 4). This apparent discrepancy could originate from the fact that crystalline Fe-sulfides might not be dissolved through the H_2O_2 extraction (Gleyzes et al., 2002). All this suggests that authigenic Fe is partly pyritized in Lake Uru Uru sediments. Additionally, and similarly to the Cala Cala Lagoon, Fe sequestration is probably achieved through the precipitation of non-sulfidic authigenic minerals such as Fe-carbonates. This process is likely favored by periodic and/or episodic re-oxidation and extended periods of suboxic conditions (Aller, 2004) that are typically encountered in the northern part of the lake due to WC evaporation. Manganese behavior contrasts with that of Fe, with no (or little) removal from porewater within the sampled depth-intervals (Fig. 5b and c) probably due to a deeper reactive zone for Mn-oxyhydroxides reduction and/or the influence of evaporation processes particularly influencing Mn as suggested by the correlation between porewater Mn with Cl^- and SO_4^{2-} (Table 6).

Similarly to the Cala Cala Lagoon, denitrification is not evidenced in Lake Uru Uru sediments (Fig. 5b and c). On the contrary, NO_3^- is produced (anaerobic nitrification) in both seasons and both northern and southern parts. This can be attributed to the reduction of Mn-oxyhydroxides by NH_4^+ (Hulth et al., 1999; Hyacinthe et al., 2001). However, it is possible that denitrification actually occurs in Lake Uru Uru while being masked by higher rates of anaerobic nitrification.

4.2. Post-depositional redistribution of trace metals and metalloids

4.2.1. The Cala Cala Lagoon

Aside from two narrow concentration peaks at 5-cm and 35-cm depth, trace metals and As exhibits rather flat porewater profiles (Fig. 6). Additionally, trace metals and metalloids, with the exception of Cd and As, are mainly associated with the residual fraction (Fig. 3 and Table 4). All this suggests low reactivity of trace element-bearing phases that induces a relatively weak post-depositional redistribution of these elements. The shallow production of dissolved Zn, Cd, Pb, U, Sb and, to a lesser extent, Cu within the SO_4 reduction zone (5 first cm) and well above the Fe- and Mn-oxyhydroxides reductive dissolution zone (20-cm depth) is attributed to release mainly from biogenic material by OM mineralization which is intense in the upper part of the profile. The release of trace elements from biogenic material into porewater during early diagenesis is in agreement with previous works reporting similar observations from freshwater environments (e.g. El Bilali et al., 2002; Audry et al., 2006b, 2010). The low contribution of Fe-oxyhydroxides to porewater trace elements is likely related to their weak reactivity suggested by the low mean contribution of reducible fraction F3 (8 ± 2%; Fig. 3). Additional mobilization along the profiles of adsorbed Cd (high mean contribution of fraction F1; Fig. 3 and Table 4) from the particulate phase is likely and controlled by the change of pH and redox associated with early diagenetic processes (Boudreau, 1997). In contrast to the other trace elements, As post-depositional redistribution is tightly linked to that of Fe. Particulate As is provided to the WSI associated with Fe- and Mn-oxyhydroxides as indicated by the high mean concentration and contribution of fraction F3 (Fig. 3 and Table 4). The release of As into the porewater just below the WSI and above the Fe- and Mn-oxyhydroxides reductive dissolution layer points to the mobilization of As bound to Fe-oxyhydroxides before Fe is reduced implying reductive desorption from Fe-oxyhydroxides rather than reductive dissolution, as reported from laboratory experiments by Masscheleyn et al. (1991) and Zobrist et al. (2000) and suggested for other freshwater systems (Audry et al., 2011).

Partial or complete removal of dissolved trace elements, with the exception of As, is observed above (Cu, Zn, U) or below (Pb,

Cd, Sb) the reduction layer of Fe- and Mn-oxyhydroxides (Fig. 6a). That points to the sequestration of Cu and Zn through the authigenic precipitation of their respective distinct sulfides rather than co-precipitation and/or sorption with Fe sulfides. Such behavior has been reported previously for other freshwater sediments (e.g. Huerta-Diaz et al., 1998). At depth, in the zone of dissolved Fe removal, the solubility of Cd and Pb is likely controlled by sorption and/or co-precipitation with Fe sulfides. Nearly complete removal of U from pore water around 15 cm depth is in agreement with the insoluble nature and very strong affinity of this element to binding sites present at the surface of particles (Klinkhammer and Palmer, 1991). The removal of U from the dissolved phase, which means the reduction of U(VI) to U(IV), is observed at the depth where SO_4 reduction is proceeding (Fig. 5a). Therefore, as suggested by Langmuir (1978), U(VI) is likely reduced by HS^- released in the pore water during SO_4 reduction. Additionally, U(VI) could be reduced to U(IV) through bacterial enzymatic reduction (Cochran et al., 1986) coupled to OM oxidation, with U acting as an electron acceptor. Indeed, some authors (Lovley and Phillips, 1992) have shown that SO_4-reducing microorganisms can effectively reduce U(VI). Therefore, the concentration-profile of dissolved U suggests that SO_4-reducing microorganisms control U release into pore water and subsequent adsorption onto particulates.

The well-resolved concave-shaped Sb profile below 5 cm depth (Fig. 6) indicates that Sb solubility is controlled by early diagenetic reactions. These processes likely involve sulfides through: (i) Sb sorption on Fe-sulfide, as proposed by Chen et al. (2003) for other freshwater lakes, and (ii) increasing production under anoxic conditions of anionic S-coordinated Sb complexes (Helz et al., 2002) that tend to condense to form large polymeric colloidal molecules (Filella et al., 2002) and tend to be retained by the 0.2 μm-porosity filters and, therefore, partly removed from porewater. In the Cala Cala Lagoon sediments, As solubility and sequestration seems not to be controlled by Fe-sulfide or clay minerals, in contrast to what has been often observed in other freshwater environments (Smedley and Kinniburgh, 2002), as evidenced by relatively high and constant (centered around 7600 nM; Fig. 6a) As concentrations in porewater.

4.2.2. Lake Uru Uru

In the mining- and smelting-impacted Lake Uru Uru, the post-depositional behavior of trace metals and metalloids is controlled by the competition between evaporation- and redox-related processes that trigger non-steady state effects, particularly in the lake's northern part. The control of evaporation is evidenced by the porewater concentrations of Cu, Zn, Cd, Pb and Sb below the detection limit in the first 2.5 cm below the WSI (Fig. 6b) in DS and the correlation of Sb and Zn with Cl^- (R^2 = 0.89; Table 6). Evaporation promotes element saturation in porewater likely triggering sorption/precipitation processes and subsequent trace element removal. With the reappearance of the WC at the end of the DS, and the subsequent onset of porewater anoxia, concentration gradients build up (Fig. 6c) due to dissolved trace element production/removal processes. Zinc, Cd, Pb and As are released just below the WSI in WS. However, due to a 'compressed' redox zonation (i.e., overlap of SO_4 reduction and Fe- and Mn-oxyhydroxide reductive dissolution zones) in comparison to the Cala Cala Lagoon, it is difficult to decipher between biogenic material and Fe- and Mn-oxyhydroxides as the carrier phases of each trace element. Arsenic is extremely responsive to the return of reducing conditions being the only trace element studied here that is released into porewater just below the WSI during DS (Fig. 6b). This is probably due to its strong association with highly reactive Fe- and Mn-oxyhydroxides (Fig. 4a and b). Higher dissolved concentrations deeper in the core during DS, as well as WS, might reflect the fact that deeper redox conditions (partial or total anoxia) are preserved, keeping reducing reactions going and keeping (part) of trace metals and metalloids in the dissolved phase. The strong removal of Cu and, to a lesser extent Sb and U, from porewater in the first cm of sediment in WS is likely the consequence of the WC re-instalment, a WC that is enriched in those three trace elements compared to the depleted shallow porewater.

In the Southern Lake Uru Uru, intense post-depositional redistribution of trace elements is promoted by highly reactive carrier phases just below the WSI (Fig. 4c and d) and high exported fluxes of biogenic material (POC) to the WSI (~6 wt.%; Fig. 2d and e). Post-depositional redistribution is fairly similar to that from the Cala Cala Lagoon: (i) release of Cu, Zn, Pb above the Fe- and Mn-oxyhydroxides reductive dissolution zone and, therefore, from biogenic material; (ii) reductive desorption of As. Antimony is released concomitantly to As and probably from the same carrier phase(s) as supported by the similar porewater profiles (R^2 = 0.80) and close particulate partitioning (Fig. 4c and d). In this part of the lake, Cu behavior is particularly controlled by OM: POC and Cu extracted by H_2O_2 (Fraction F4) are correlated over both cores (R^2 = 0.82 in DS and 0.74 in WS). Uranium is likely linked to the Mn cycle and controlled by Mn-oxyhydroxide reductive dissolution, as suggested by correlated U and Mn porewater concentrations in DS (R^2 = 0.72) and reported for other continental environments (Swarzenski et al., 1999; Elbaz-Poulichet et al., 2005). Trace element solubility and sequestration at depth are likely controlled by Fe-sulfides present in the sediment and containing As (up to 0.2 wt.% as revealed by electron microprobe analysis; Fig. 7a and b) and Cu for instance (Fig. 7c). This is in accordance with data reported for other mining-impacted freshwater sediments (Audry et al., 2010). Additional control of trace element sequestration at depth in the sediment is likely provided by authigenesis of non-sulfidic minerals such as Fe-rich and Mn-rich carbonates as suggested by the non-negligible concentrations of trace elements in the NaOAc fraction (F2; Table 4).

5. Environmental concerns and concluding remarks

The lacustrine sediments of the Altiplano of Oruro are affected by multiple and complex early diagenetic processes (Fig. 8). These sediments are characterized by a high demand for electron acceptors, with reduction of SO_4 and Fe- and Mn-oxyhydroxides representing the main pathways of OM anaerobic mineralization. Climatic seasonal variability exerts a strong influence on diagenetic processes and trace element post-depositional redistribution by promoting non-steady-state geochemical conditions and, therefore, unsteady diagenetic regimes at the water–sediment interface and below in the sediments. These unsteady diagenetic regimes are well illustrated by the strong seasonal variability of the intensity of diffusive transport through the water–sediment interface (Table 5). Evaporation of surface water during the dry season in the northern part of Lake Uru Uru, weakening of anoxia conditions in near-surface sediments, promotes large redox front oscillations in the sediments, increases the residence time of the sediment in the oxic zone promoting the oxidation of reduced minerals (Fe-sulfides) and formation of oxidized precipitates. It also favors the coexistence of Fe-oxyhydroxides alongside Fe-sulfides in the sediment and the non-equilibrium rate of Fe-sulfide formation in the sediment. In contrast, increased residual deposits of fresh OM at the water–sediment interface following algal bloom periods might strengthen the anoxia conditions. Seasonal disappearance of the WC in Northern Lake Uru Uru entails an alternation of: (i) low trace element mobility in the dry season due to elemental precipitation, (ii) increased trace element mobility via diffusive transport during the wet season due to their release from OM, Fe- and Mn-oxyhydroxides and carbonates upon mineralization, reductive

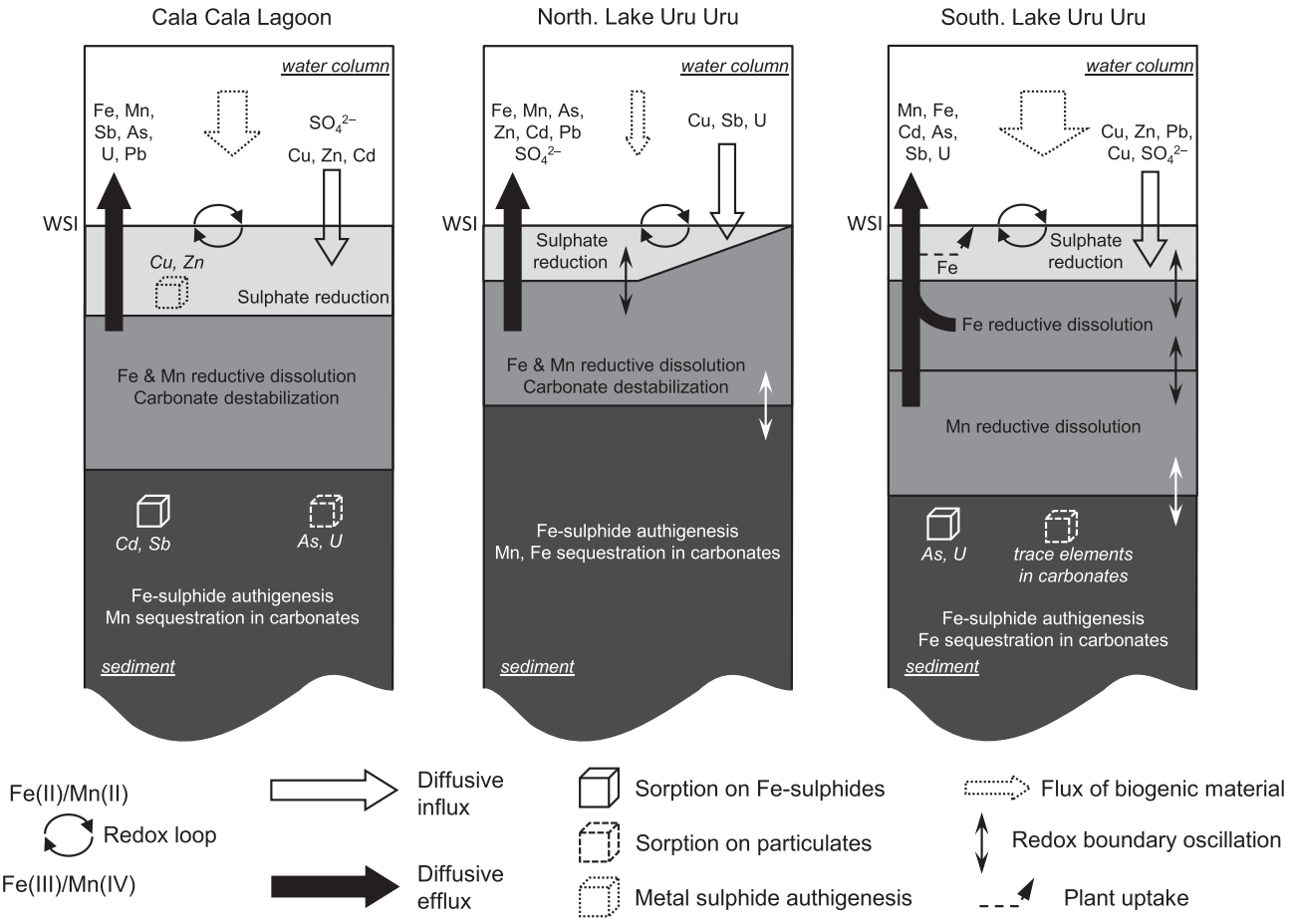

Fig. 8. Schematic depiction of the main early diagenesis processes and the associated post-depositional redistribution and sequestration of trace metals and metalloids in the sediments of the Cala Cala Lagoon and Lake Uru Uru. WSI, water–sediment interface.

dissolution and destabilization processes, respectively. Re-oxidation of authigenic Fe-sulfides likely following the re-instalment of the WC above the sediment at the end of the dry season and prior to the return of anoxia probably favors trace element mobility and their transport to the WC. This is supported by the porewater concentration gradients (Fig. 6) and diffusional transport (Table 5) that indicate that trace elements (particularly Cd and As) are not immediately sequestrated in an insoluble form (e.g. sulfides). The non-steady-state, by maintaining relatively high concentrations of trace elements in porewater, is likely the main factor controlling trace element mobility. Both northern and southern sediments are mainly a source of dissolved trace elements, particularly As, for the overlying WC (Fig. 8). Intensive recycling of As but changing redox conditions at the water–sediment interface likely controls the proportions of As eventually buried associated with Fe-sulfides, As transported to the overlying bottom water and As trapped in the redox loop associated with Fe- and Mn-oxyhydroxide recycling. Using the annual rates of diffusive transport through the water–sediment interface (Table 5) and integrating them over the surface areas represented by the northern (90 km^2) and southern (60 km^2) give 381, 364, and 54 tons of Mn, Fe and As, respectively, that would be transferred annually to the overlying WC. However, taking into account the redox loop that promotes precipitation of authigenic Fe- and Mn-oxyhydroxides near the water–sediment interface and assuming a maximum incorporation of As into freshly precipitated Fe-oxyhydroxides of 15 wt.% (Rancourt et al., 2001; Zhao et al., 2011), all of the As (as well as Cd) added to the WC by diffusive transport could be removed from the WC and redistributed to the particulate phase. This could be considered as a natural mitigation process, shielding the water column from dissolved As and Cd accumulation.

Finally, sequestration of trace metals and metalloids in the sediments is likely partly controlled by inter-annual climate variability, i.e. ENSO events. It is expected that, in extremely rainy years (La Niña events), anoxia conditions prevail in the sediments, favoring sustained diffusive transport of trace metals and metalloids to the WC as well as sequestration associated with authigenic Fe-sulfides. In contrast, extreme aridity (El Niño events), by weakening the reductive conditions in the sediments, should favor the sequestration of trace metals and metalloids by Fe- and Mn-oxyhydroxides. In the long term, owing the more frequent occurrences of El Niño events during the past few decades and the projected more frequent El-Niño-like conditions (Timmermann et al., 1999), enhanced and more perennial trace element sequestration in sediments should take place, hence mitigating the impact of mining- and smelting-derived metals and metalloids on the lacustrine ecosystems of the Bolivian Altiplano.

The data set show that an intricate web of redox- and climate-related processes have a considerable affect on the time and space redistribution of metal and metalloid contaminants in the Uru Uru lacustrine ecosystem. Government environmental regulators and/or mining industry environmental coordinators could use this knowledge to push for environmentally conscious solutions in the Bolivian Altiplano. The current approach, implemented by the Government of Bolivia in 2009 seems to favor short-term (3–4 years) tailings retention, particularly in the Huanuni watershed. However, as long as mining and smelting activities still go on in the Bolivian Altiplano, sediment and water quality of Lake

Uru Uru are not expected to recover naturally. Sustained inputs of suspended material and water from mining, ore-treatment and untreated waste-dumping sites, will maintain high particulate and dissolved fluxes of contaminants. Due to the mineralized nature of Lake Uru Uru's geological surroundings, natural particles are enriched in trace elements compared to the UCC. Therefore, the deposition of natural particles at the water–sediment interface cannot be considered as an efficient dilution process that would progressively lower significantly the contaminant concentrations in the sediment.

Additionally, the findings point toward the accumulation of As-rich particles (see Fig. 4) precipitated through the redox loop in the top sediment layers of Lake Uru Uru. This fact should be taken into account by government environmental bodies as a potential environmental threat: during the dessication episodes affecting the northern part of the lake, particularly, the erosive action of the wind could generate airborne particles. Because aerosols, particularly fine ones, enriched in metal contaminants, promote acute respiratory effects (Schwartz and Neas, 2000) and the main wind direction is from the south during the dry season in the Oruro district (Goix et al., 2011), sediment particles from the northern part of Lake Uru Uru could be eroded and transported to the city of Oruro. This is of great concern as the city of Oruro is already heavily impacted by aerosols enriched in As, Cd and Sb originating from smelting activities (Goix et al., 2011).

Acknowledgments

This study would have not been possible without the help provided by the following individuals in the GET: Frédéric Candaudap and Aurélie Lanzanova for the ICP-MS analyses; Jonathan Prunier, Manuel Henry and Carole Boucayrand for the sediment digestions. During the Bolivian field campaigns, we received valuable help from Jean-Louis Duprey, Jacques Gardon, Marcelo Claure, Abdul Castillo, and Patrick Blanchon. We also thank the staff of the UMSA (Universidad Mayor de San Andrés): J. César Calderón, Lincy Ugarte, Erika Paty, Carla Ibáñez, Carlos Molina and Samantha, and Mr. Carlos Wayta, of Oruro, for their presence in the field campaigns and their valuable help during the coring campaigns. Pr. Brian Townley is acknowledged for valuable discussions during the preparation of this manuscript. Insightful comments from two anonymous reviewers are gratefully acknowledged. J. Tapia benefitted from PhD grants from CONYCIT (D-21070053) and IRD (625890E).

References

Alborès, A.F., Cid, B.P., Gómez, E.F., López, E.F., 2000. Comparison between sequential extraction procedures and single extractions for metal partitioning in sewage sludge samples. Analyst 125, 1353–1357.

Allen, J.R.L., Rae, J.E., Zanin, P.E., 1990. Metal speciation (Cu, Zn, Pb) and organic matter in an oxic salt marsh, Severn Estuary, southwest Britain. Mar. Pollut. Bull. 21, 574–580.

Aller, R.C., 1990. Bioturbation and manganese cycling in hemipelagic sediments. Philos. Trans. Roy. Soc. London 331, 51–68.

Aller, R.C., 1994. The sedimentary Mn cycle in Long Island Sound: its role as intermediate oxidant and the influence of bioturbation, O_2 and C_{org} flux on diagenetic reaction balances. J. Mar. Res. 52, 259–295.

Aller, R.C., 2004. Conceptual models of early diagenetic processes: the muddy seafloor as an unsteady, batch reactor. J. Mar. Res. 62, 815–835.

Aller, R.C., Rude, P.D., 1988. Complete oxidation of solid phase sulfides by manganese and bacteria in anoxic marine sediments. Geochim. Cosmochim. Acta 52, 751–765.

Aller, R.C., Heilbrun, C., Panzeca, C., Zhu, Z., Baltzer, F., 2004. Coupling between sedimentary dynamics, early diagenetic processes, and biogeochemical cycling in the Amazon-Guianas mobile mud belt: coastal French Guiana. Mar. Geol. 208, 331–360.

Arce-Burgoa, O., Goldfarb, R., 2009. Metallogeny of Bolivia. In: Society of Economic Geologists Newsletter. <http://www.osvaldoarce.com/Metallogeny.html>.

Audry, S., Blanc, G., Schafer, J., 2006a. Solid state partitioning of trace metals in suspended particulate matter from a river system affected by smelting-waste drainage. Sci. Total Environ. 363, 216–236.

Audry, S., Blanc, G., Schäfer, J., Chaillou, G., Robert, S., 2006b. Early diagenesis of trace metals (Cd, Cu, Co., Ni, U, Mo, and V) in the freshwater reaches of a macrotidal estuary. Geochim. Cosmochim. Acta 70, 2264–2282.

Audry, S., Blanc, G., Schäfer, J., Guérin, F., Masson, M., Robert, S., 2007. Budgets of Mn, Cd and Cu in the macrotidal Gironde estuary (SW France). Mar. Chem. 107, 433–448.

Audry, S., Grosbois, C., Bril, H., Schäfer, J., Kierczak, J., Blanc, G., 2010. Post-depositional redistribution of trace metals in reservoir sediments of a mining/smelting-impacted watershed (the Lot River, SW France). Appl. Geochem. 25, 778–794.

Audry, S., Pokrovsky, O.S., Shirokova, L.S., Kirpotin, S.N., Dupré, B., 2011. Organic matter mineralization and trace element post-depositional redistribution in Western Siberia thermokarst lake sediments. Biogeosciences 8, 3341–3358.

Berner, R.A., 1980. Early Diagenesis: A Theoretical Approach. Princeton University Press, New York.

Böttcher, M.E., Thamdrup, B., 2001. Anaerobic sulfide oxidation and stable isotope fractionation associated with bacterial sulfur disproportionation in the presence of MnO_2. Geochim. Cosmochim. Acta 65, 1573–1581.

Boudreau, B.P., 1996. The diffusive tortuosity of fine-grained unlithified sediments. Geochim. Cosmochim. Acta 60, 3139–3142.

Boudreau, B.P., 1997. Diagenetic Models and their Implementations: Modeling Transport and Reactions in Aquatic Sediments. Springer, Berlin, Heidelberg, NY.

Boudreau, B.P., 1999. Metals and models: diagenetic modelling in freshwater lacustrine sediments. J. Paleolimnol. 22, 227–251.

Calvert, S.E., Pedersen, T.F., 1993. Geochemistry of recent oxic and anoxic marine sediments: implications for the geological record. Mar. Geol. 113, 67–88.

Canavan, R.W., Van Cappellen, P., Zwolsman, J.J.G., van den Berg, G.A., Slomp, C.P., 2007. Geochemistry of trace metals in a fresh water sediment: field results and diagenetic modeling. Sci. Total Environ. 381, 263–279.

Chaillou, G., Anschutz, P., Lavaux, G., Schäfer, J., Blanc, G., 2002. The distribution of Mo, U, and Cd in relation to major redox species in muddy sediments of the Bay of Biscay. Mar. Chem. 80, 41–59.

Chen, Y.W., Deng, T.L., Filella, M., Belzile, N., 2003. Distribution and early diagenesis of antimony species in sediments and porewaters of freshwater lakes. Environ. Sci. Technol. 37, 1163–1168.

Cochran, J.K., Carey, A.E., Sholkovitz, E.R., Surprenant, L.D., 1986. The geochemistry of uranium and thorium in coastal marine sediments and sediment pore waters. Geochim. Cosmochim. Acta 50, 663–680.

Davison, W., 1993. Iron and manganese in lakes. Earth-Sci. Rev. 34, 119–163.

De Lange, G.J., 1986. Early diagenetic reactions in interbedded pelagic and turbiditic sediments in the Nares Abyssal Plain (western North Atlantic): consequences for the composition of sediment and interstitial water. Geochim. Cosmochim. Acta 50, 2543–2561.

Dill, H.G., 1998. Evolution of Sb mineralisation in modern fold belts: a comparison of the Sb mineralisation in the Central Andes (Bolivia) and the Western Carpathians (Slovakia). Mineral. Depos. 33, 359–378.

El Bilali, L., Rasmussen, P.E., Hall, G.E.M., Fortin, D., 2002. Role of sediment composition in trace metal distribution in lake sediments. Appl. Geochem. 17, 1171–1181.

Elbaz-Poulichet, F., Seidel, J.L., Jezequel, D., Metzger, E., Prevot, F., Simonucci, C., Sarazin, G., Viollier, E., Etcheber, H., Jouanneau, J.-M., 2005. Sedimentary record of redox-sensitive elements (U, Mn, Mo) in a transitory anoxic basin (the Thau lagoon, France). Mar. Chem. 95, 271–281.

Filella, M., Belzile, N., Chen, Y.-W., 2002. Antimony in the environment: a review focused on natural waters: II. Relevant solution chemistry. Earth-Sci. Rev. 59, 265–285.

Froelich, P.N., Klinkhammer, G.P., Bender, M.L., Luedtke, N.A., Heath, G.R., Cullen, D., Dauphin, P., Hammond, D., Hartman, B., Maynard, V., 1979. Early oxidation of organic matter in pelagic sediments of the eastern equatorial Atlantic: suboxic diagenesis. Geochim. Cosmochim. Acta 43, 1075–1090.

Garcia Moreno, M.E., 2006. Transport of Arsenic and Heavy Metals to lake Poopó–Bolivia – Natural Leakage and Anthropogenic Effects. PhD Dissertation. Department of Water Resources Engineering. Lund Univ.

Gehler, E., 1984. Comportamiento de *Schoenoplectus totora* (totora) frente al hierro y plata en soluciones acuosas. Rev. Boliviana Química 5, 21–31.

Gleyzes, C., Tellier, S., Astruc, M., 2002. Fractionation studies of trace elements in contaminated soils and sediments: a review of sequential extraction procedures. TRAC. Trends Anal. Chem. 21, 451–467.

Gobeil, C., Macdonald, R.W., Sundby, B., 1997. Diagenetic separation of cadmium and manganese in suboxic continental margin sediments. Geochim. Cosmochim. Acta 61, 4647–4654.

Goix, S., Point, D., Oliva, P., Polve, M., Duprey, J.L., Mazurek, H., Guislain, L., Huayta, C., Barbieri, F.L., Gardon, J., 2011. Influence of source distribution and geochemical composition of aerosols on children exposure in the large polymetallic mining region of the Bolivian Altiplano. Sci. Total Environ. 412–413, 170–184.

Granina, L., Muller, B., Wehrli, B., 2004. Origin and dynamics of Fe and Mn sedimentary layers in Lake Baikal. Chem. Geol. 205, 55–72.

Helz, G.R., Valerio, M.S., Capps, N.E., 2002. Antimony speciation in alkaline sulfide solutions: role of zerovalent sulfur. Environ. Sci. Technol. 36, 943–948.

Huerta-Diaz, M.A., Tessier, A., Carignan, R., 1998. Geochemistry of trace metals associated with reduced sulfur in freshwater sediments. Appl. Geochem. 13, 213–233.

Hulth, S., Aller, R.C., Gilbert, F., 1999. Coupled anoxic nitrification/manganese reduction in marine sediments. Geochim. Cosmochim. Acta 63, 49–66.

Hyacinthe, C., Van Cappellen, P., 2004. An authigenic iron phosphate phase in estuarine sediments: composition, formation and chemical reactivity. Mar. Chem. 91, 227–251.
Hyacinthe, C., Anschutz, P., Carbonel, P., Jouanneau, J.-M., Jorissen, F.J., 2001. Early diagenetic processes in the muddy sediments of the Bay of Biscay. Mar. Geol. 177, 111–128.
Klinkhammer, G.P., Palmer, M.R., 1991. Uranium in the oceans: where it goes and why. Geochim. Cosmochim. Acta 55, 1799–1806.
Kostka, J.E., Luther III, G.W., 1994. Partitioning and speciation of solid phase iron in saltmarsh sediments. Geochim. Cosmochim. Acta 58, 1701–1710.
Kufel, L., Kufel, I., 2002. Chara beds acting as nutrient sinks in shallow lakes—a review. Aquat. Bot. 72, 249–260.
Langmuir, D., 1978. Uranium solution-mineral equilibria at low temperatures with applications to sedimentary ore deposits. Geochim. Cosmochim. Acta 42, 547–569.
Laslett, R.E., Balls, P.W., 1995. The behaviour of dissolved Mn, Ni and Zn in the forth an industrialised, partially mixed estuary. Mar. Chem. 48, 311–328.
Lavenu, A., Fornari, M., Sebrier, M., 1984. Existence de deux nouveaux episodes lacustres quaternaires dans l'Altiplano Peróu-Bolivien. Cahiers ORSTOM. ser. Geol. 14, 103–114.
Lee, G., Bigham, J.M., Faure, G., 2002. Removal of trace metals by coprecipitation with Fe, Al and Mn from natural waters contaminated with acid mine drainage in the Ducktown Mining District, Tennessee. Appl. Geochem. 17, 569–581.
Lesven, L., Gao, Y., Billon, G., Leermakers, M., Ouddane, B., Fischer, J.C., Baeyens, W., 2008. Early diagenetic processes aspects controlling the mobility of dissolved trace metals in three riverine sediment columns. Sci. Total Environ. 407, 447–459.
Li, Y.-H., Gregory, S., 1974. Diffusion of ions in sea water and in deep-sea sediments. Geochim. Cosmochim. Acta 38, 703–714.
Lovley, D.R., Phillips, E.J., 1992. Reduction of uranium by Desulfovibrio desulfuricans. Appl. Environ. Microbiol. 58, 850–856.
Ma, Y.B., Uren, N.C., 1995. Application of a new fractionation scheme for heavy metals in soils. Commun. Soil Sci. Plant Anal. 26, 3291–3303.
Malea, P., Boubonari, T., Kevrekidis, T., 2008. Iron, zinc, copper, lead and cadmium contents in Ruppia maritima from a Mediterranean coastal lagoon: monthly variation and distribution in different plant fractions. Bot. Mar. 51, 320–330.
Masscheleyn, P.H., Delaune, R.D., Patrick, W.H., 1991. Effect of redox potential and pH on arsenic speciation and solubility in a contaminated soil. Environ. Sci. Technol. 25, 1414–1419.
Morford, J.L., Emerson, S., 1999. The geochemistry of redox sensitive trace metals in sediments. Geochim. Cosmochim. Acta 63, 1735–1750.
Morford, J.L., Emerson, S.R., Breckel, E.J., Kim, S.H., 2005. Diagenesis of oxyanions (V, U, Re, and Mo) in pore waters and sediments from a continental margin. Geochim. Cosmochim. Acta 69, 5021–5032.
Petersen, W., Willer, E., Willamowski, C., 1997. Remobilization of trace elements from polluted anoxic sediments after resuspension in oxic water. Water Air Soil Pollut. 99, 515–522.
Postma, D., Jakobsen, R., 1996. Redox zonation: equilibrium constraints on the Fe(III)/SO_4-reduction interface. Geochim. Cosmochim. Acta 60, 3169–3175.
PPO, 1993–1996. Proyecto Piloto Oruro. Ministerio de Desarrollo Sostenible y Medio Ambiente Secretaría Nacional de Minería, Swedish Geological AB.
PPO-9606, 1996. Proyecto Piloto Oruro: Hydrology of the PPO Area. Ministerio de Desarrollo Sostenible y Medio Ambiente Secretaría Nacional de Minería, Swedish Geological AB.
Quevauviller, P., 1998. Operationally defined extraction procedures for soil and sediment analysis I. Standardization. TrAC, Trends Anal. Chem. 17, 289–298.
Rancourt, D.G., Fortin, D., Pichler, T., Thibault, P.-J., Lamarche, G., Morris, R.V., Mercier, P.H.J., 2001. Mineralogy of a natural As-rich hydrous ferric oxide coprecipitate formed by mixing of hydrothermal fluid and seawater: implications regarding surface complexation and color banding in ferrihydrite deposits. Am. Mineral. 86, 834–851.
Risacher, F., Fritz, B., 1991. Quaternary geochemical evolution of the salars of Uyuni and Coipasa, Central Altiplano, Bolivia. Chem. Geol. 90, 211–231.
Rosenberg, E., Ariese, F., 2001. Quality control in speciation analysis. In: Rosenberg, E., Ariese, F. (Eds.), Trace Element Speciation for Environment, Food and, Health, pp. 17–50.
Rosenthal, Y., Lam, P., Boyle, E.A., Thomson, J., 1995. Authigenic cadmium enrichments in suboxic sediments: precipitation and postdepositional mobility. Earth Planet. Sci. Lett. 132, 99–111.
Schäfer, J., Blanc, G., Lapaquellerie, Y., Maillet, N., Maneux, E., Etcheber, H., 2002. Ten-year observation of the Gironde tributary fluvial system: fluxes of suspended matter, particulate organic carbon and cadmium. Mar. Chem. 79, 229–242.
Schwartz, J., Neas, L.M., 2000. Fine particles are more strongly associated than coarse particles with acute respiratory health effects in schoolchildren. Epidemiology 11, 6–10.
Slomp, C.P., Malschaert, J.F.P., Lohse, L., Van Raaphorst, W., 1997. Iron and manganese cycling in different sedimentary environments on the North Sea continental margin. Cont. Shelf Res. 17, 1083–1117.
Smedley, P.L., Kinniburgh, D.G., 2002. A review of the source, behaviour and distribution of arsenic in natural waters. Appl. Geochem. 17, 517–568.
Soto-Jiménez, M.F., Páez-Osuna, F., 2008. Diagenetic processes on metals in hypersaline mudflat sediments from a subtropical saltmarsh (SE Gulf of California): postdepositional mobility and geochemical fractions. Appl. Geochem. 23, 1202–1217.
Suits, N.S., Arthur, M.A., 2000. Bacterial production of anomalously high dissolved sulfate concentrations in Peru slope sediments: steady-state sulfur oxidation, or transient response to end of El Nino? Deep Sea Res. Part I: Oceanog. Res. Papers 47, 1829–1853.
Sundby, B., Martinez, P., Gobeil, C., 2004. Comparative geochemistry of cadmium, rhenium, uranium, and molybdenum in continental margin sediments. Geochim. Cosmochim. Acta 68, 2485–2493.
Swarzenski, P.W., McKee, B.A., Skei, J.M., Todd, J.F., 1999. Uranium biogeochemistry across the redox transition zone of a permanently stratified fjord: Framvaren, Norway. Mar. Chem. 67, 181–198.
Tack, F.M.G., Vossius, H.A.H., Verloo, M.G., 1996. A comparison between sediment metal fractions, obtained from sequential extraction and estimated from single extractions. Int. J. Environ. Anal. Chem. 63, 61–66.
Tack, F.M.G., Vossius, H.A.H., Verloo, M.G., 1999. Single extractions versus sequential extraction for the estimation of heavy metal fractions in reduced and oxidised dredged sediments. Chem. Spec. Bioavail. 11, 43–50.
Tang, D., Warnken, K.W., Santschi, P.H., 2002. Distribution and partitioning of trace metals (Cd, Cu, Ni, Pb, Zn) in Galveston Bay waters. Mar. Chem. 78, 29–45.
Tapia, J., Audry, S., Townley, B., Duprey, J.L., 2012. Geochemical background, baseline and origin of contaminants from sediments in the mining-impacted Altiplano and Eastern Cordillera of Oruro, Bolivia. Geochem. Explor. Environ. Anal. 12, 3–20.
Tessier, A., Campbell, P.G.C., Bisson, M., 1979. Sequential extraction procedure for the speciation of particulate trace metals. Environ. Sci. Technol. 51, 844–851.
Timmermann, A., Oberhuber, J., Bacher, A., Esch, M., Latif, M., Roeckner, E., 1999. Increased El Niño frequency in a climatemodel forced by future greenhouse warming. Nature 398, 694–697.
Tromp, T.K., Van Cappellen, P., Key, R.M., 1995. A global model for the early diagenesis of organic carbon and organic phosphorus in marine sediments. Geochim. Cosmochim. Acta 59, 1259–1284.
UNEP, 1996. Diagnóstico Ambiental del Sistema TDSP. División de Aguas Continentales de las Naciones Unidas para el Medio Ambiente.
Van Cappellen, P., Viollier, E., Roychoudhury, A., Clark, L., Ingal, E., Lowe, K., Dichristina, T., 1998. Biogeochemical cycles of manganese and iron at the oxic–anoxic transition of a stratified marine basin (Orca Basin, Gulf of Mexico). Environ. Sci. Technol. 32, 2931–2939.
Wang, Y., Van Cappellen, P., 1996. A multicomponent reactive transport model of early diagenesis: application to redox cycling in coastal marine sediments. Geochim. Cosmochim. Acta 60, 2993–3014.
Wedepohl, H.K., 1995. The composition of the continental crust. Geochim. Cosmochim. Acta 59, 1217–1232.
Whiteley, J.D., Pearce, N.J.G., 2003. Metal distribution during diagenesis in the contaminated sediments of Dulas Bay, Anglesey, N. Wales, UK. Appl. Geochem. 18, 901–913.
Widerlund, A., Ingri, J., 1995. Early diagenesis of arsenic in sediments of the Kalix River estuary, northern Sweden. Chem. Geol. 125, 185–196.
Zhao, Z., Jia, Y., Xu, L., Zhao, S., 2011. Adsorption and heterogeneous oxidation of As(III) on ferrihydrite. Water Res. 45, 6496–6504.
Zobrist, J., Dowdle, P.R., Davis, J.A., Oremland, R.S., 2000. Mobilisation of arsenite by dissimilatory reduction of adsorbed arsenate. Environ. Sci. Technol. 34, 4747–4753.